中国科学院国家天文台
National Astronomical Observatories, CAS

the SILK ROAD PROJECT at NAOC
丝绸之路 计划

Star Cluster Dynamics
Gravitational Waves
GPU Supercomputing

Uni Heidelberg

Rainer Spurzem with Silk Road Team

National Astronomical Observatories (NAOC),
Key Lab Computational Astrophysics, Chinese Academy of Sciences
Astronomisches Rechen-Inst., ZAH, Univ. of Heidelberg, Germany
Kavli Institute for Astronomy and Astrophysics (KIAA), Peking University

Here main collaborators:

Peter Berczik (NAOC/MAO/Heidelberg)
Long Wang (now Japan-former KIAA/PKU)
M.B.N. Kouwenhoven (now Suzhou XJTLU-former KIAA/PKU)
Sverre Aarseth (Inst. Of Astron. U Cambridge, UK)
T. Naab, R. Schadow (MPA Garching),
M. Giersz, A. Askar (CAMK Warsaw)

VolkswagenStiftung

spurzem@nao.cas.cn
http://silkroad.bao.ac.cn

Our Main Research Projects are:

- Binary Supermassive Black Holes and Gravitational Waves in Quiet and Active Galactic Nuclei

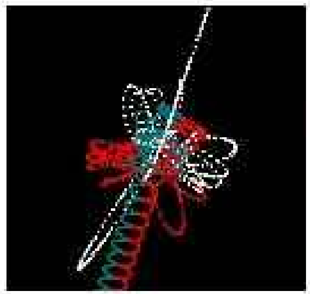
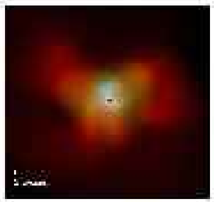


- Dynamical Evolution of Stars and Gas in Galactic Nuclei and Dense Star Clusters
- How are planetary systems forming and evolving (in star clusters)?
- How can we design supercomputers which are faster and consume less energy?

ICCS
International Center for Computational Science


千人計畫
RECRUITMENT
PROGRAM OF GLOBAL EXPERTS

Support and Collaboration by CNIC @ NAOC (Chenzhou CUI and team)

- Education and Workshops in Computational and Theoretical Astrophysics, Parallel Programming and Accelerated Computing

the SILK ROAD PROJECT at NAOC/KIAA
丝绸之路 计划

RECRUITMENT
PROGRAM OF GLOBAL EXPERTS

Pictures from:
http://www.chinatourselect.com/

http://silkroad.bao.ac.cn

National Astron. Observatory of Chinese Academy of Sciences, Beijing China
Kavli Institute for Astronomy and Astrophysics, Peking University, Beijing, China
Fesenkov Astrophysical Institute, Space Institute, Almaty, Kazakhstan
Institute of Space Technology, Islamabad, Pakistan (NEW)
Main Astronomical Observatory of Ukrainian Academy of Sciences, Kiev, Ukraine
Astrophysical Institute Univ. of Vienna, Austria
Astronomisches Rechen-Institut,Zentrum f. Astronomie (ZAH) and
Computer Engineering and Architecture (ZITI), Univ. Of Heidelberg, Germany
Max-Planck Institute for Astrophysics (MPA), Garching/Munich, Germany

- **Instruments (Hardware/Software)**
- **Dragon Simulations of Star Clusters**
- **Black Holes / Gravitational Waves**

GPU Computing

General Purpose
GPU Supercomputing (GPGPU)

http://www.nvidia.com
http://www.astrogpu.org

http://gpgpu.org

PCI Express 2.0

NVIDIA TESLA with CUDA

GPU

- Number of processor cores: 240
- Processor core clock: 1.296 GHz
- Voltage: 1.1875 V
- Package size: 45.0 mm × 45.0 mm 2236-pin flip-chip ball grid array (FCBGA)

Board

- Fourteen layer printed circuit board (PCB)
- PCI Express 2.0 ×16 system interface
- Physical dimensions: 4.376 inches × 10.50 inches, dual slot
- Board power dissipation: 187.8 W

External Connectors

- None

Internal Connectors and Headers

- One 6-pin PCI Express power connector
- One 8-pin PCI Express power connector
- 4-pin fan connector

NVIDIA Tesla C1060
in kolob cluster Heidelberg Univ.

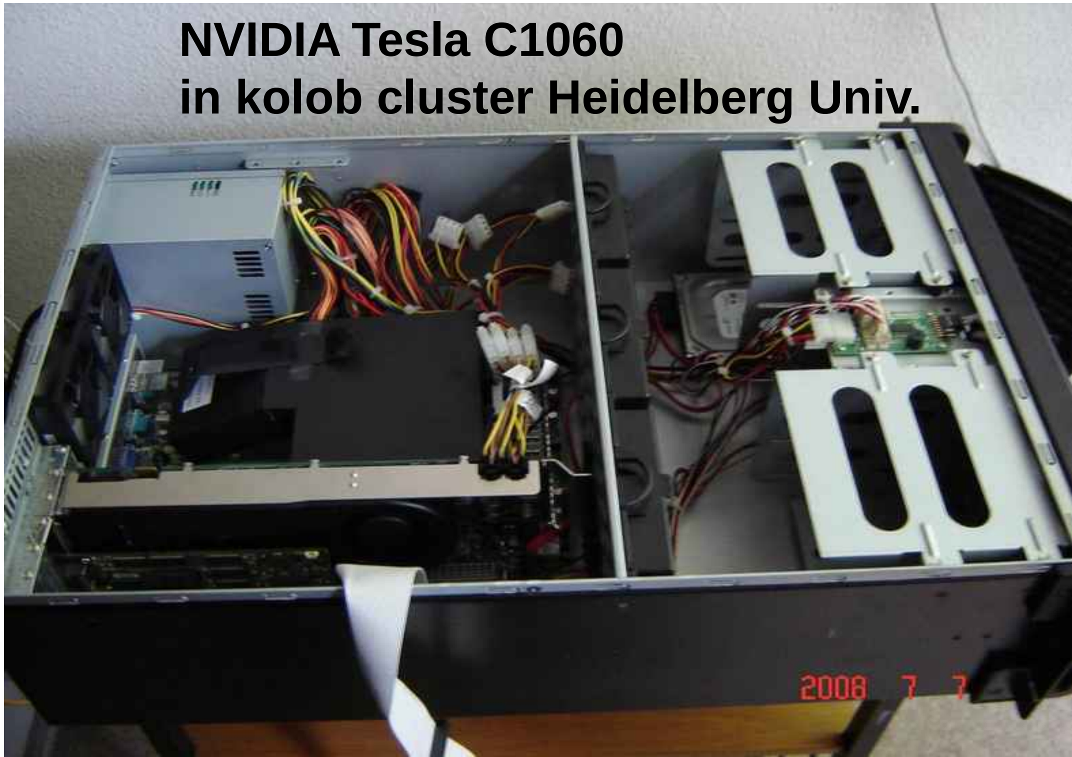

Our Green Grid: GPU Clusters used:

老虎 Beijing *(NAOC/CAS and Silk Road Project)*

85 Nodes, 64 Kepler K2

Max-Planck MPCDF GPU cluster (400 Kepler K20 GPUs)

Golowood cluster, Main Astron. Observatory, Kiev, Ukraine

Kepler cluster Heidelberg, Germany (12x Kepler GPU)

NAOC laohu cluster

64 Kepler K20

Request:
New and/or upgrade of laohu

Laohu: 2009/2013
(Kepler GPU)
100 Tflop/s 150k cores

Need for GW research:
~100 Pascal GPU
1.5 Pflop/s 300k cores

Compare:
AEI Hannover B. Allen

MPG Garching Hydra

Kepler Scaling, it works...

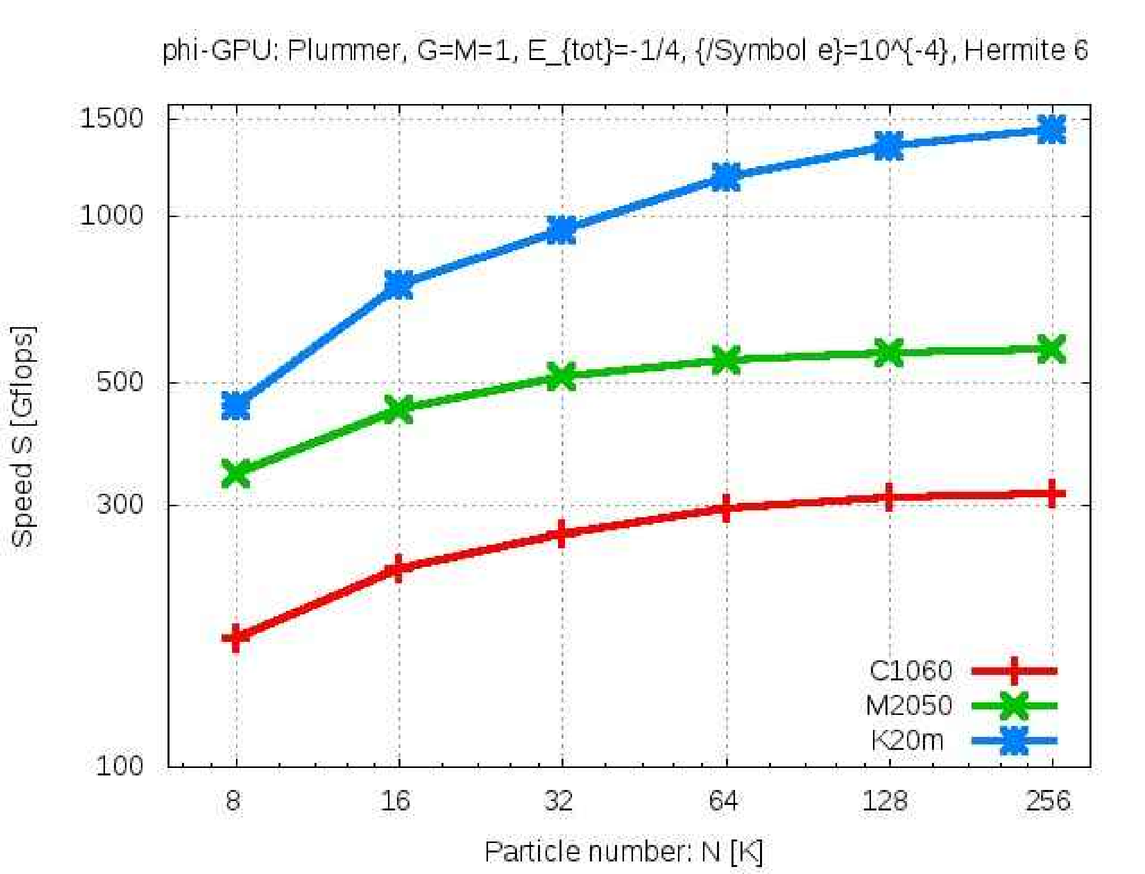

Fig. 4. Here we report a preliminary result from a benchmark test of our code on one Kepler K20 card; we compare with the performance on Fermi C2050 (used in the Mole-8.5 cluster), and the oldest Tesla C1060 GPU (used in the laohu cluster of 2009) - the latter is used as a normalization reference. We plot the speed ratio of our usual benchmarking simulation used in the previous figures, as a function of particle number. From this we see the sustained performance of a Kepler K20 would be about 1.4 - 1.5 Tflop/s.

Spurzem, Berczik, et al., 2013, LNCS Supercomputi 2013, pp. 13-25, Springer publisher.

Pascal Scaling, it works...

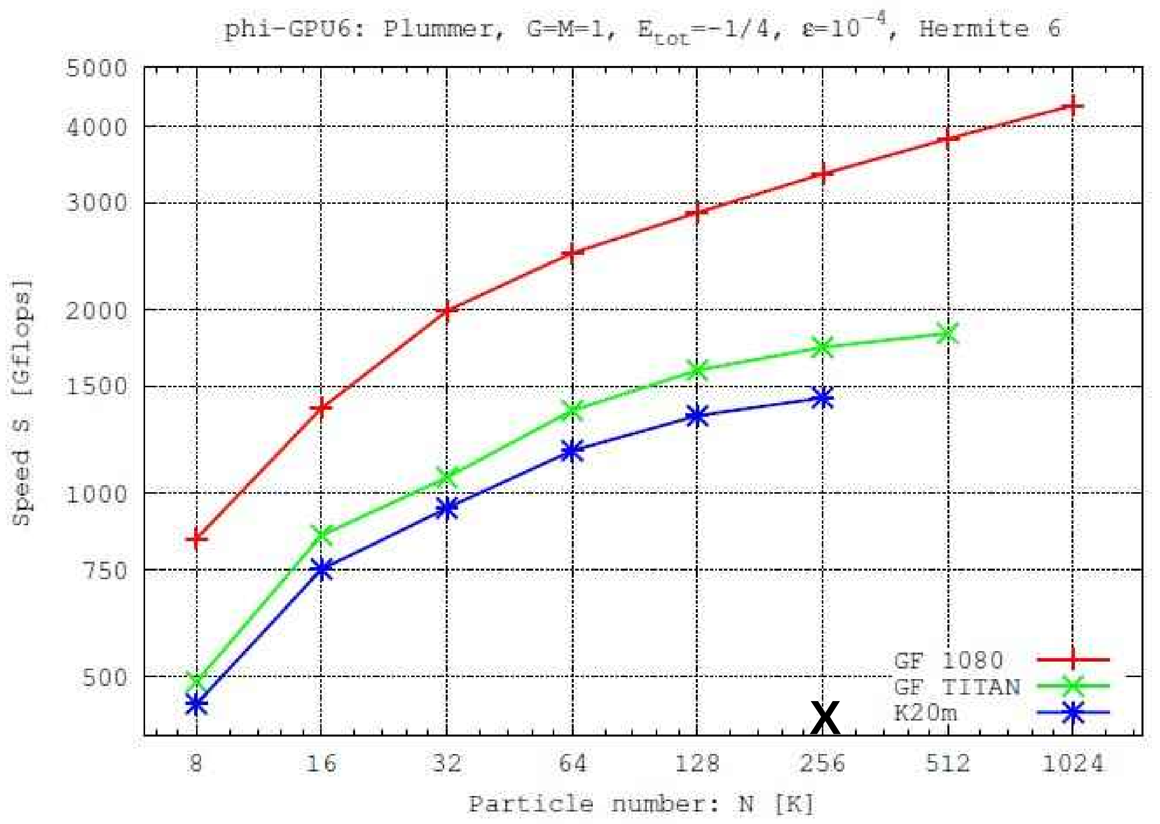

Pascal GF1080

TITAN (Kepler)

Kepler K20m

Spurzem, Berczik, et al., 2013, LNCS Supercomputing, 2013, pp. 13-25, Springer publisher.

Fig. 4. Here we report a preliminary result from a benchmark test of our code on one Kepler K20 card; we compare with the performance on Fermi C2050 (used in the Mole-8.5 cluster), and the oldest Tesla C1060 GPU (used in the laohu cluster of 2009) - the latter is used as a normalization reference. We plot the speed ratio of our usual benchmarking simulation used in the previous figures, as a function of particle number. From this we see the sustained performance of a Kepler K20 would be about 1.4 - 1.5 Tflop/s.

X = first GPU of laohu 2010

Nr. 1,2 Supercomputer from China: 96/33 Pflop/s Linpac
Wuxi/Guangzhou/Tianjin National Supercomputing Cen
Taihu 10 mill. cores

32000 Intel Xeon 12 core,
48000 Intel Phi Accelerators 57 Core

Test of Taihu planned;
But:
Local cluster with new GPUs at NAOC gives much more

Intel MIC Hardware

INSPUR, NAOC - 2013.XI.26

icpc … "-mmic" … 61 x 4 = 244 x 1.1 GHz omp cores !!!

Full fp64 !!!

PRACE

PRACE Award - 2011

Astrophysical Particle Simulations with Large Custom GPU Clusters on Three Continents

Rainer Spurzem, *et al*, Chinese Academy of Sciences & University of Heidelberg

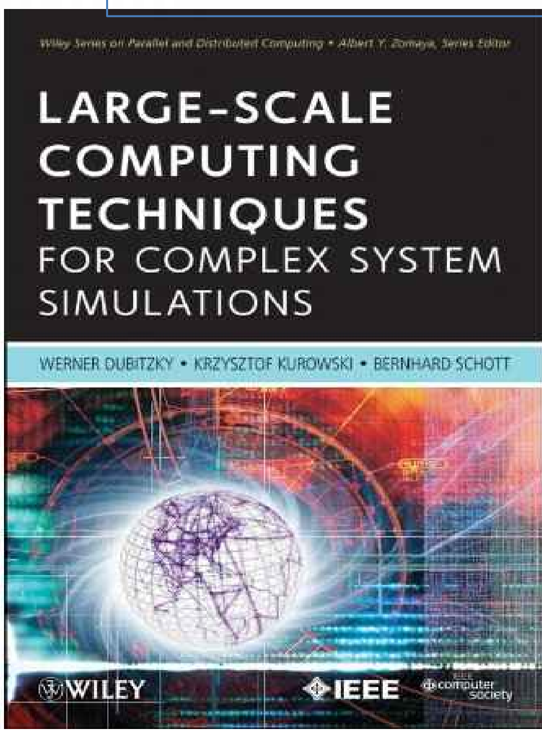

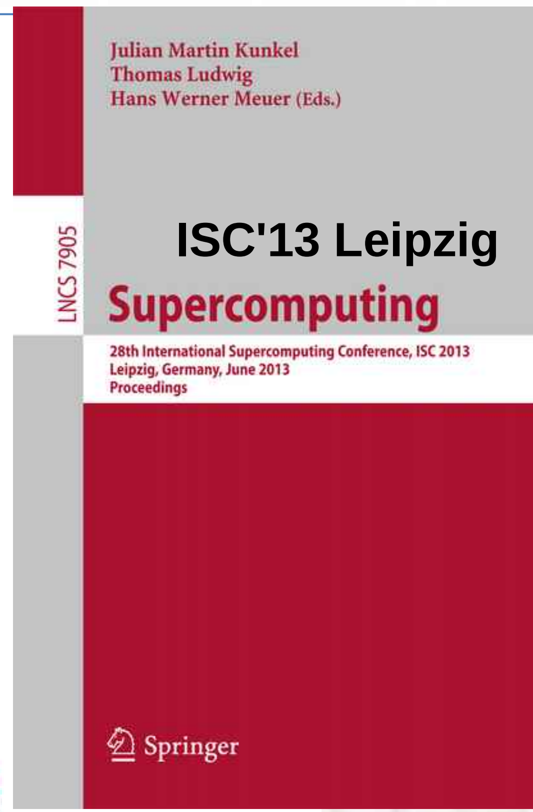

NAOC 中国科学院国家天文台

NATIONAL ASTRONOMICAL OBSERVATORIES ,CHINESE ACADEMY OF SCIENCES

北京大学 PEKING UNIVERSITY

Software

NBODY4, NBODY6, S.J.Aarseth, S. Mikkola, ...

(ca. 20.000 lines, since 1963):

- **Hierarchical Individual Time Steps (HITS)**
- **Ahmad-Cohen Neighbour Scheme (ACS)**
- **Kustaanheimo-Stiefel and Chain-Regular. (KSREG) for bound subsystems of N<6 (Quaternions!)**
- **4th order Hermite scheme (pred/corr), Bulirsch-Stoer (for Chain)**
- **Stellar Evolution (single/binary) (w Hurley)**

•***NBODY6++GPU, φGPU, L. Wang, R. Spurzem, P. Berczik, K. Nitadori,...***

- ***(massively parallel codes, since 1999, recent paper Wang, Spurzem, Aarseth, et al. 2015):***
- **NBODY6++ (Spurzem 1999) using MPI**
- **Parallel φGRAPE / φGPU (Harfst et al. 2006, Spurzem et al. 2009)**
- **NBODY6++/GPU-MPI (Wang, Spurzem, Aarseth, et al. 2015)**
- **Parallel Binary Integration in Progress (KSREG)**

Our CPU/GPU N-body (AC) code

NBODY6++GPU

Wang, Spurzem, Aarseth, et al. 2015, 2016
→ Exaflop/s Huang, Berczik, Spurzem 2016
Typical: 8/16 GPUs → 19000/38000 cores

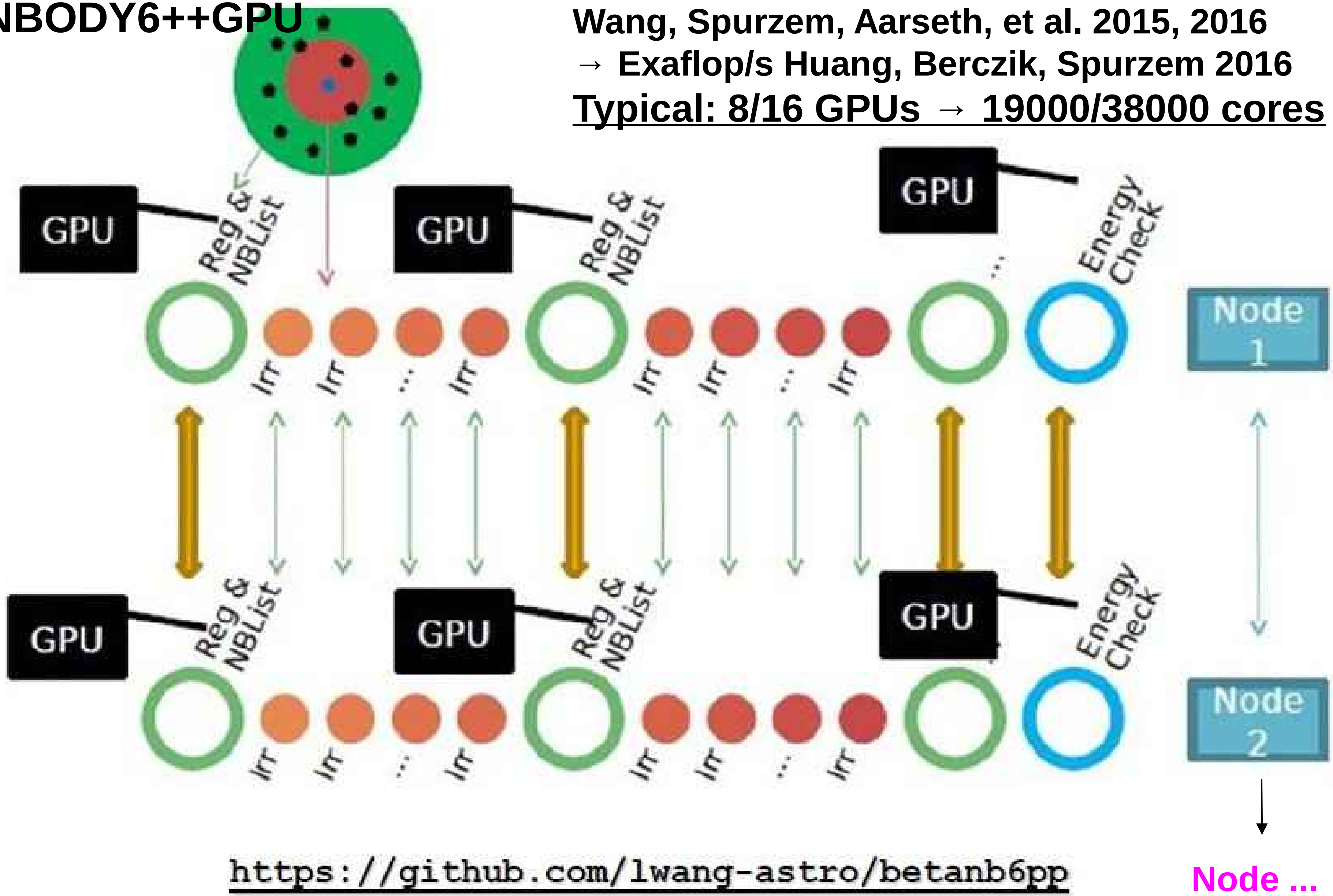

https://github.com/lwang-astro/betanb6pp

NBODY6++

PERFORMANCE OF HYBRID MPI

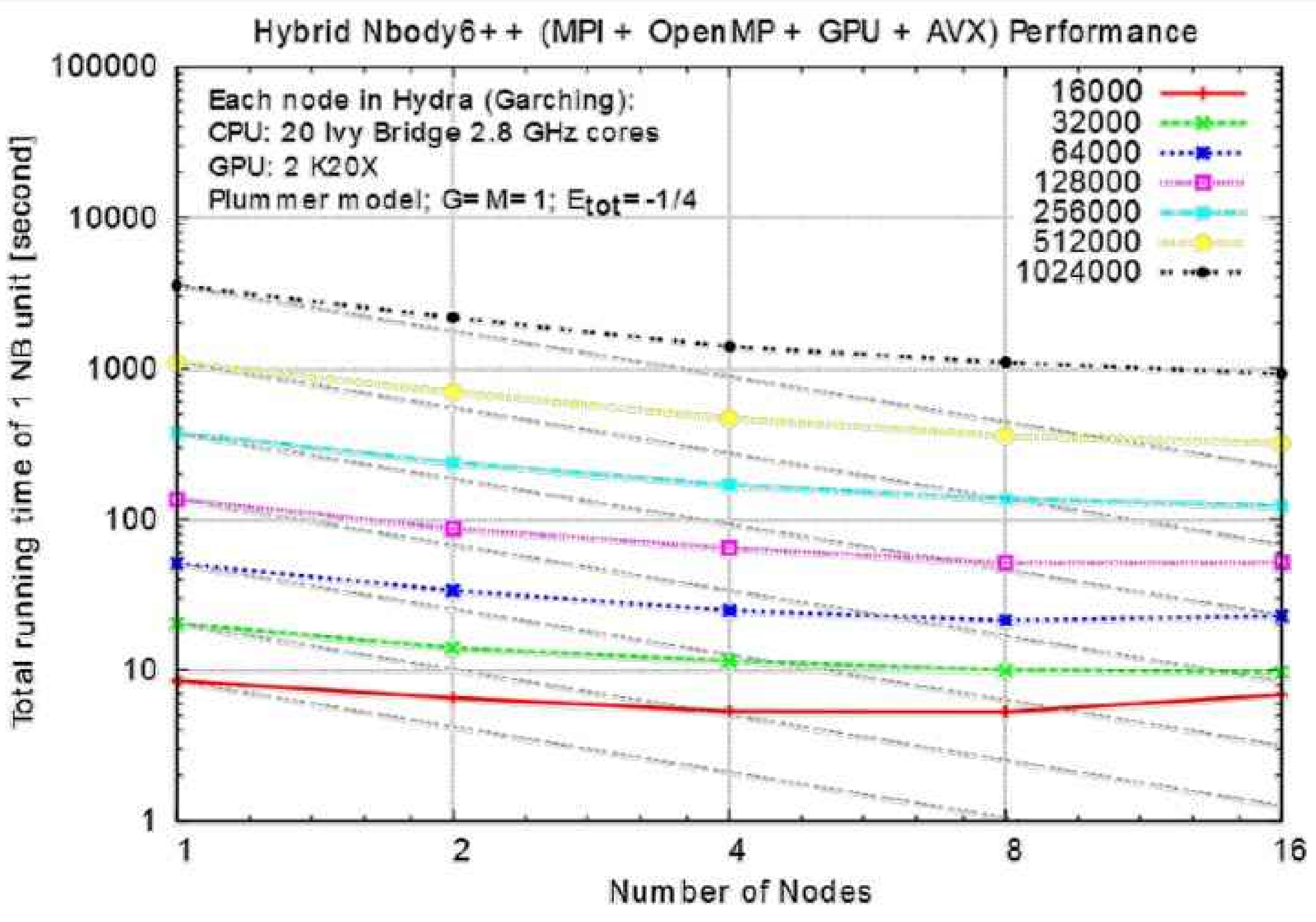

To Exaflop/s

With NBODY6++ left

With Bonsai down

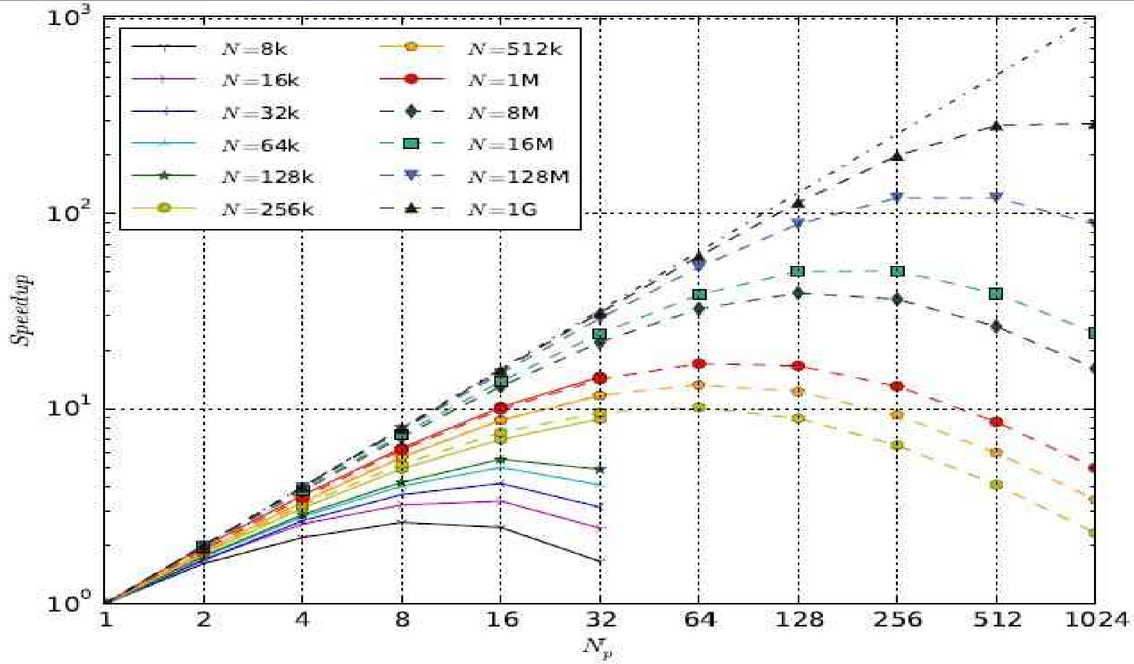

Fig. 2 The speed-up (S) of NBODY6++ as a function of particle number (N) and processor number (N_p). Solid points are the measured speed-up ratio between sequential and parallel wall-clock time, dash lines predict the performance of larger scale simulations further. The symbols used in figure have the magnitudes: $1k = 1,024$, $1M = 1k^2$ and $1G = 1k^3$.

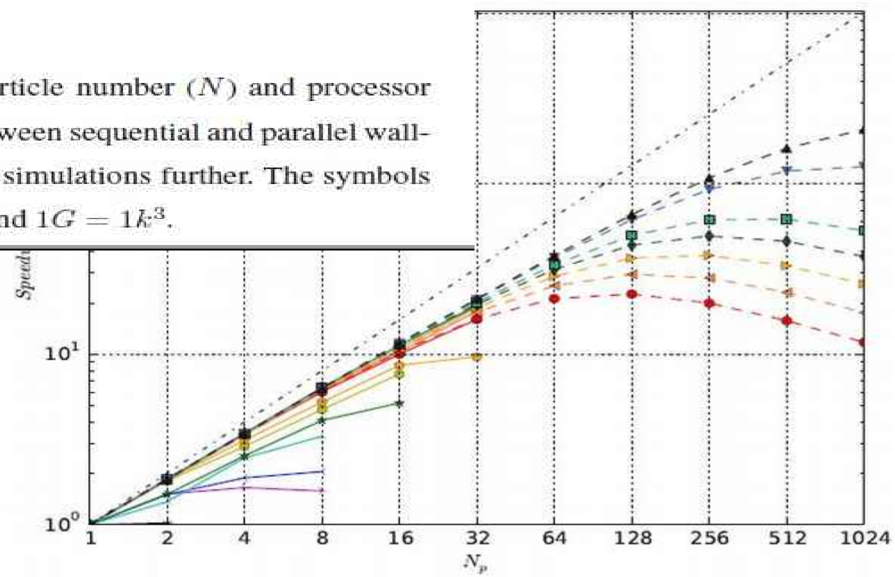

Fig. 5 The speed-up (S) of Bonsai as a function of particle number (N) and processor number (N_p). Solid points are the measured speed-up ratio between sequential and parallel wall-clock time, dash lines predict the performance of larger scale simulations further. The symbols used in figure have the magnitudes: $1k = 1,024$, $1M = 1k^2$ and $1G = 1k^3$.

Huang, Berczik, Spurzem, RAA, 2015

"Moore's" Law for Direct N-Body

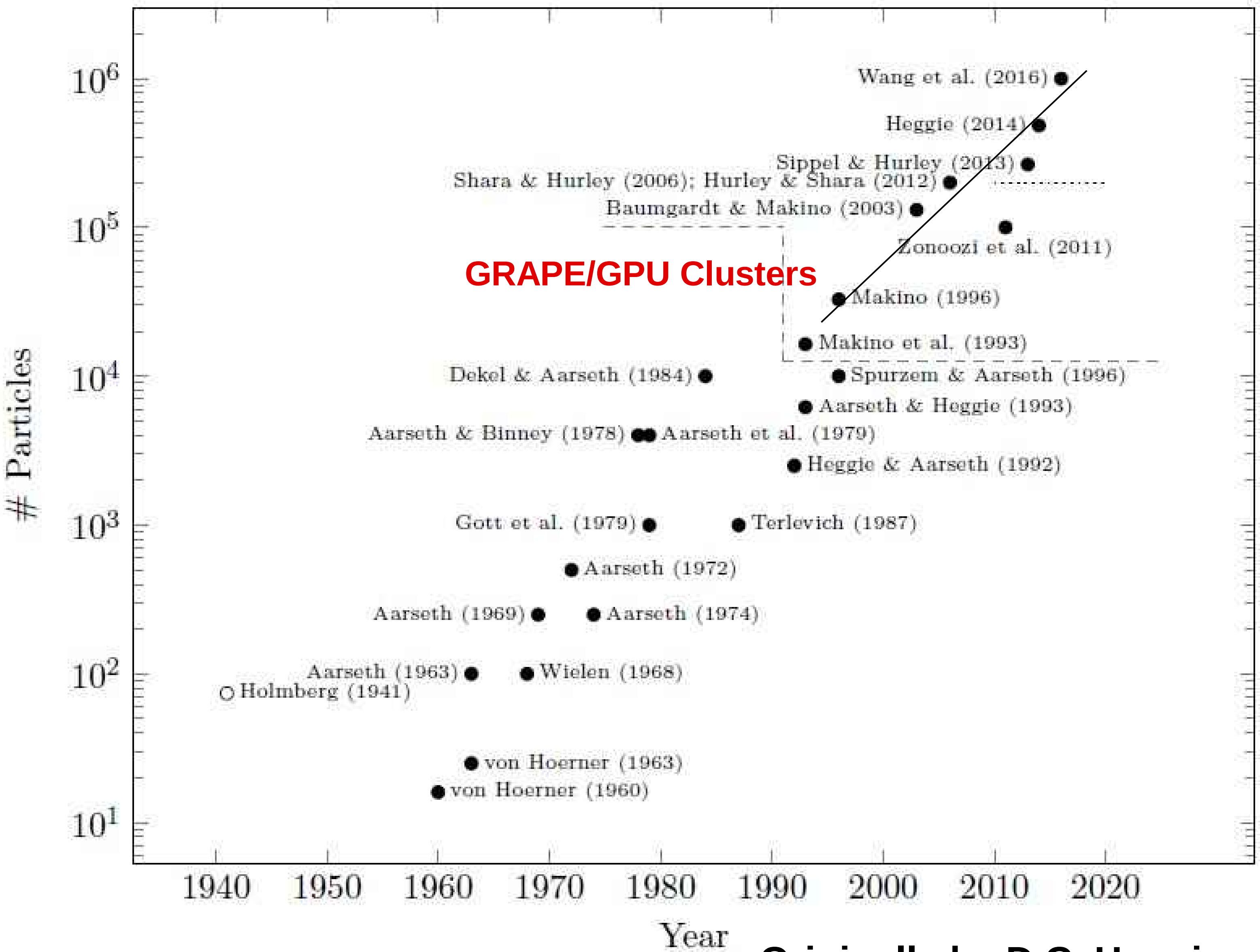

Originally by D.C. Heggie
Extended by Anna Sippel

- **Instruments (Hardware/Software)**
- **<u>Dragon Simulations of Star Clusters</u>**
- **Black Holes / Gravitational Waves**

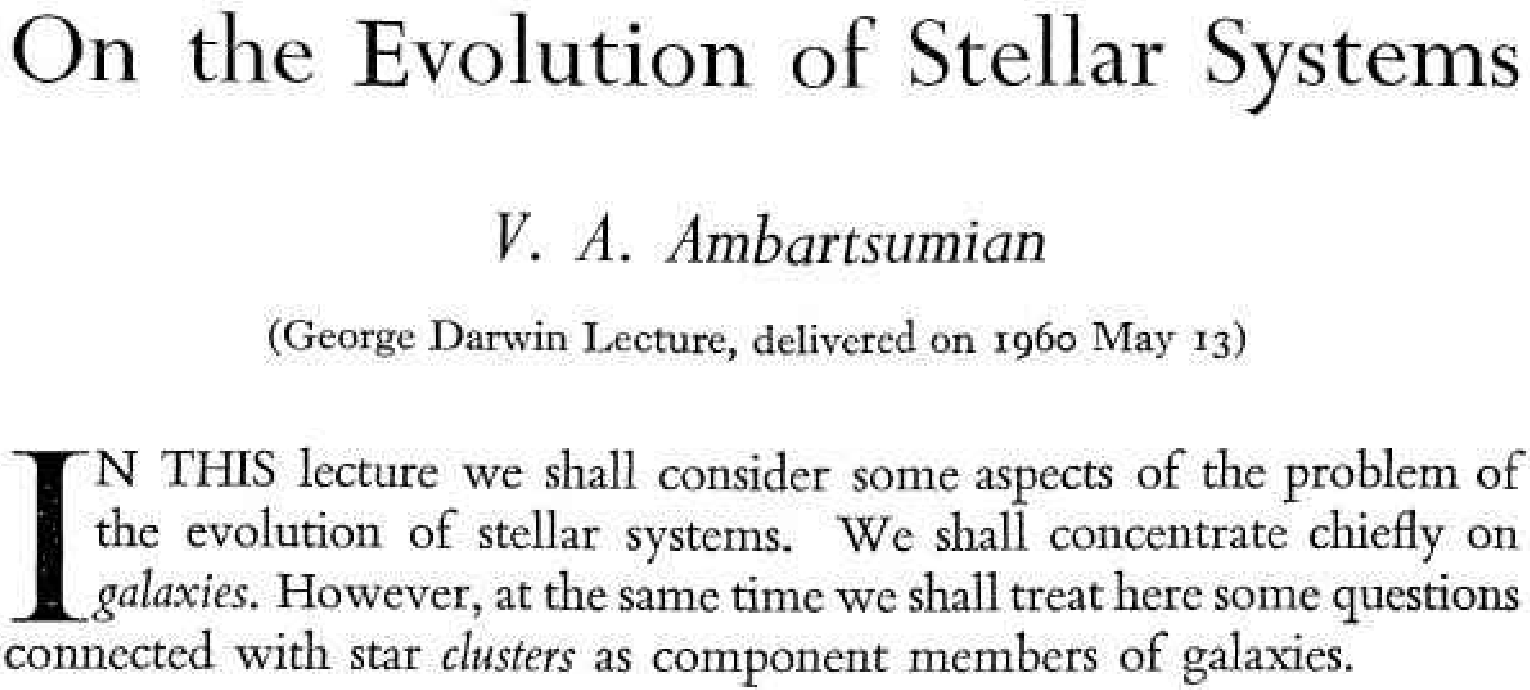

Concepts discussed:

Total Energy of grav. star clusters NOT additive

No thermodynamical equilibrium

Statistical Theory of Gases to be used with care

(large mean free path)

Locally truncated Maxwellian distribution.

$$\vec{a}_0 = \sum_j G m_j \frac{\vec{R}_j}{R_j^3} \quad ; \quad \dot{\vec{a}}_0 = \sum_j G m_j \left[\frac{\vec{V}_j}{R_j^3} - \frac{3(\vec{V}_j \cdot \vec{R}_j)\vec{R}_j}{R_j^5} \right]$$

Globular Cluster 47 Tucanae

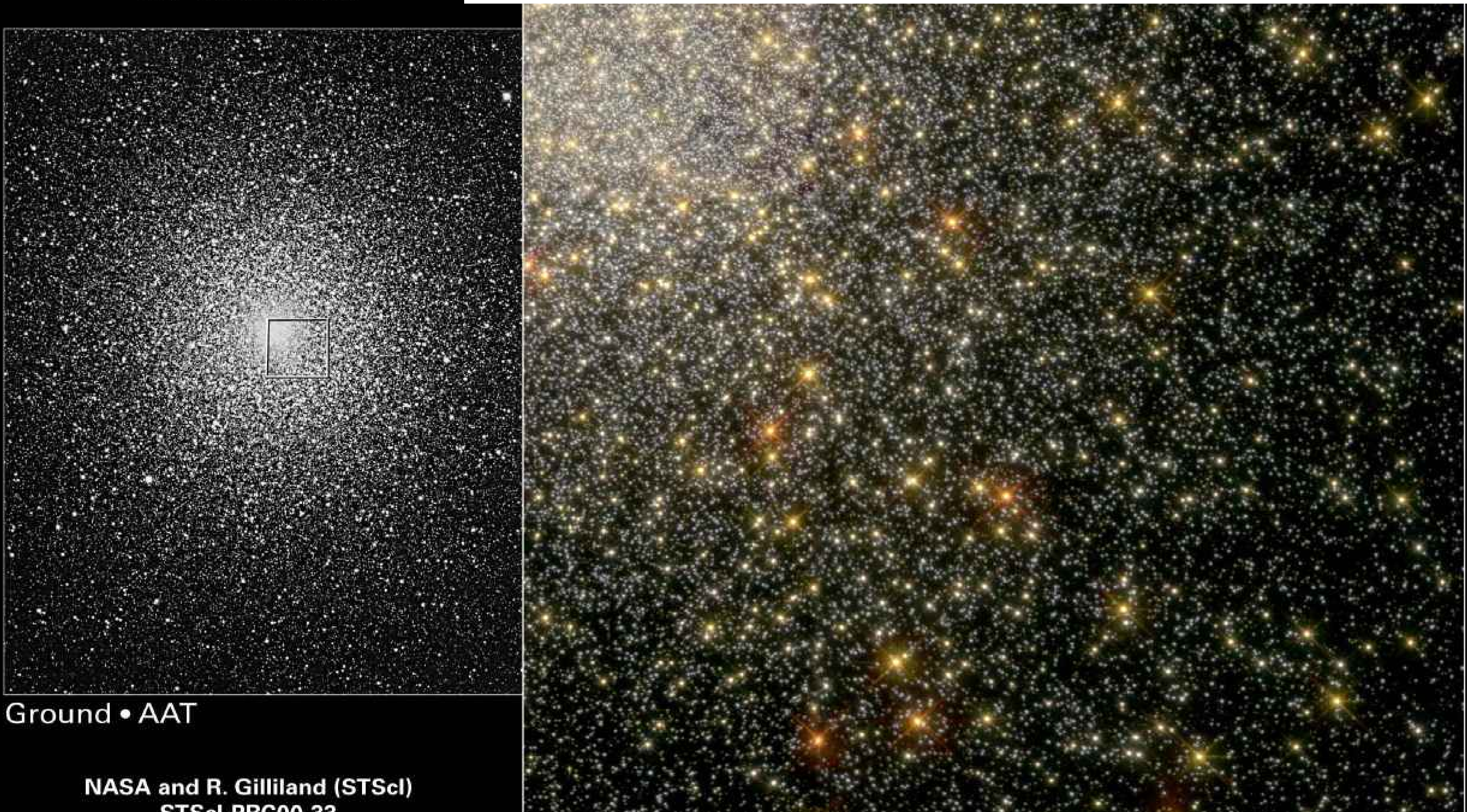

Ground • AAT

Hubble Space Telescope • WFPC2

NASA and R. Gilliland (STScI)
STScI-PRC00-33

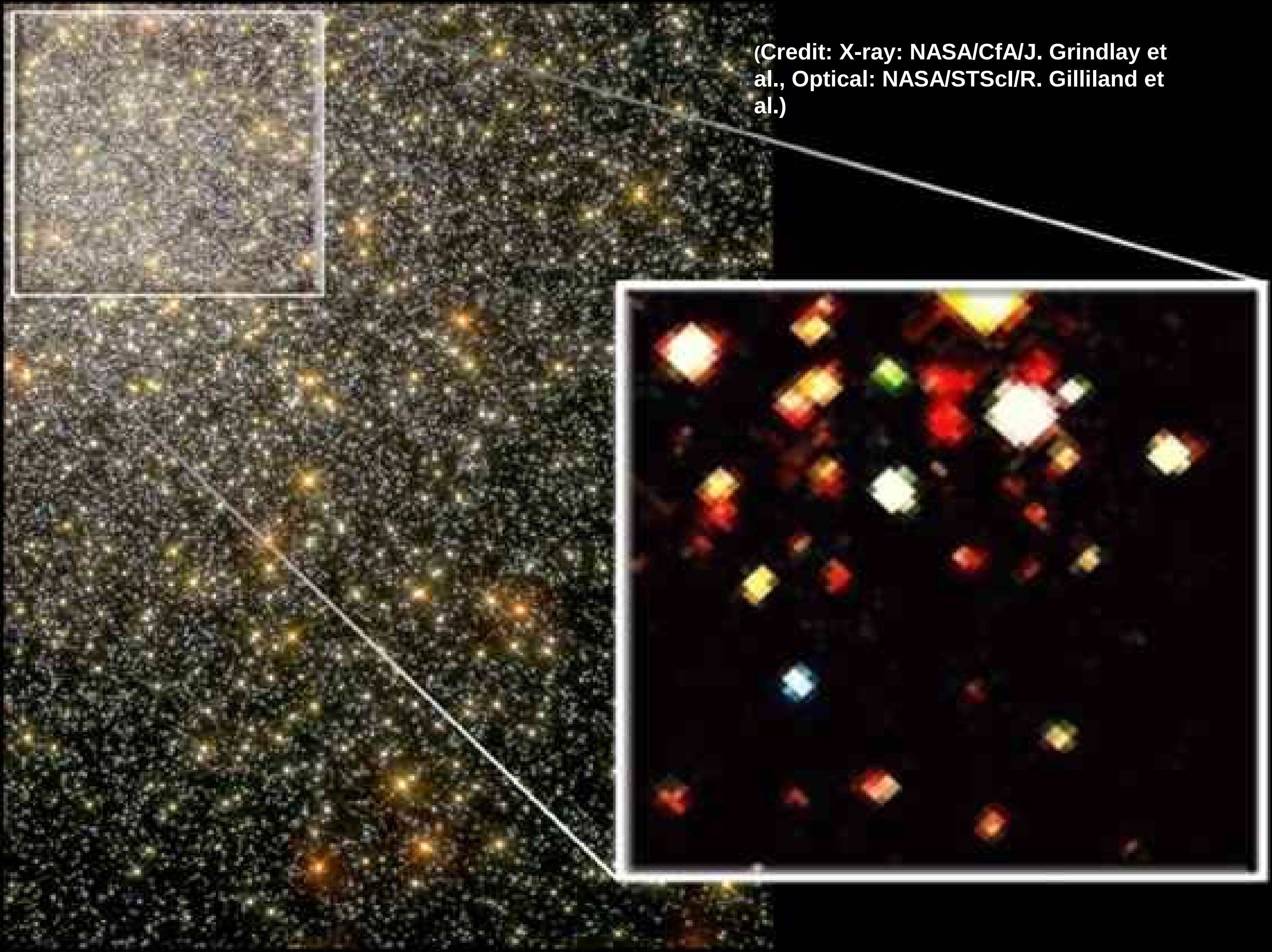

(Credit: X-ray: NASA/CfA/J. Grindlay et al., Optical: NASA/STScI/R. Gilliland et al.)

Approx. Models: Fluid Dynamics/Fokker-Planck

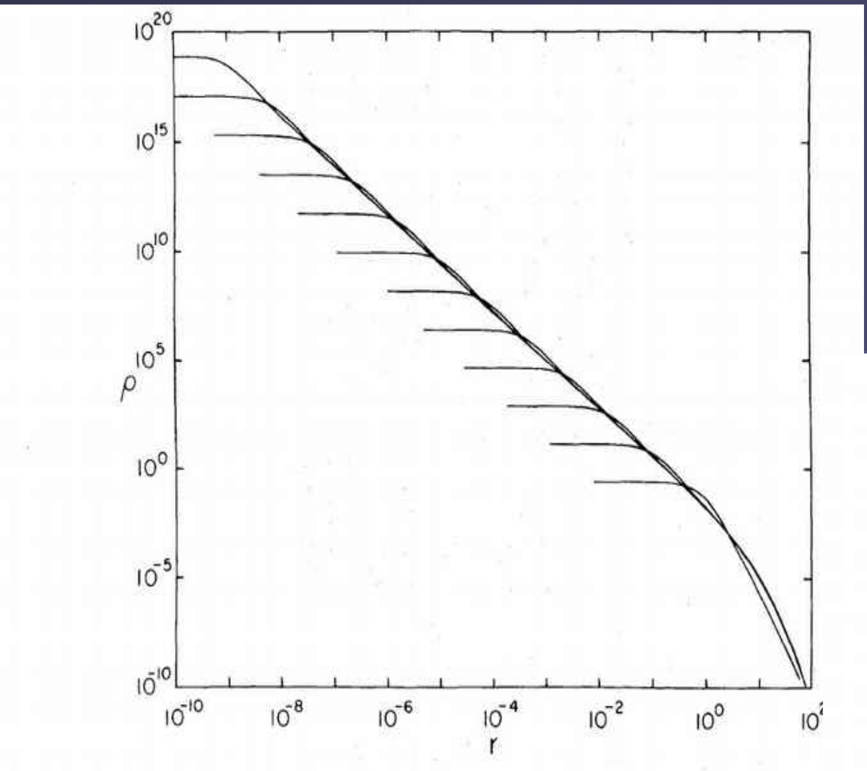

Cohn (1980): Direct Fokker-Planckj model

Core Collapse

Gravothermal Catastrophe

Bettwieser & Sugimoto 1984:

Gravothermal Oscillations by

energy generation from binaries

(cf. nuclear stellar energy generation)

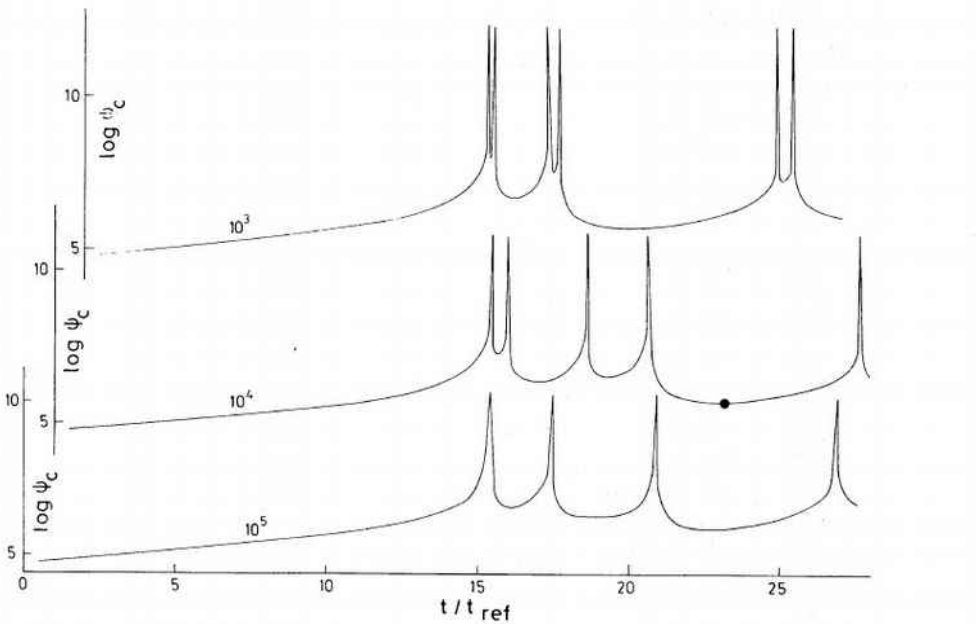

Figure 1. The 'central' density ψ_c is plotted against the non-dimensional time t/t_{ref} for $k = 2$ models with three different values of C as attached to each curve. Note, that if they were plotted with the same ordinate they would be close to each other despite the great differences in C. The model indicated with a filled circle will be compared with King's model in Section 4.2.

3-body Encounters Starlab Simulation (S.L.W. McMillan)

http://www.physics.drexel.edu/~steve/

-> Three-Body-Problem

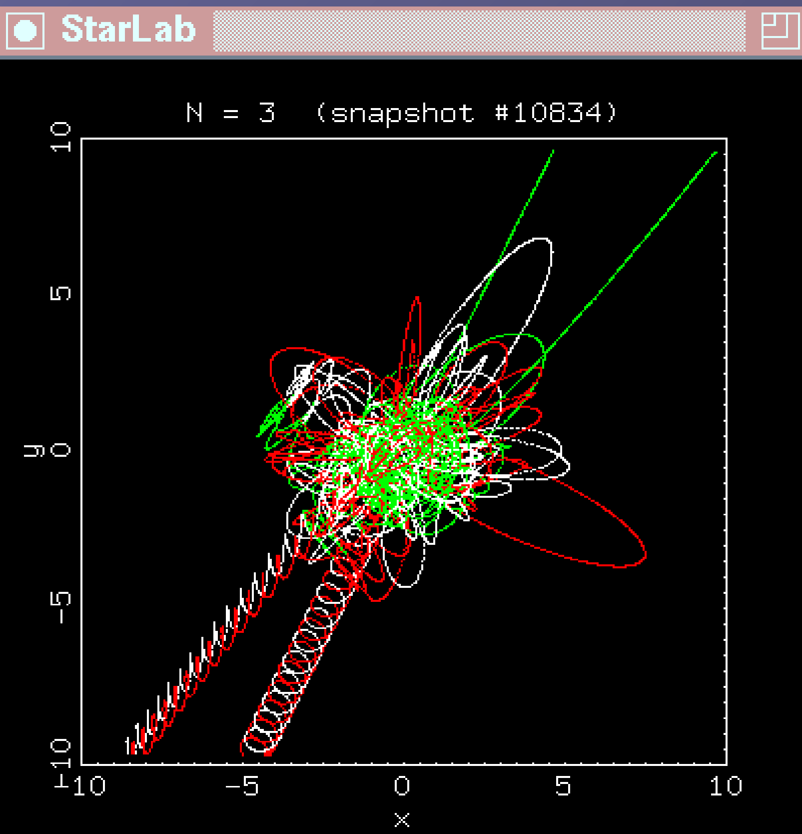

Gravothermal Oscillations - Attractor in Phase Space

Spurzem 1994, Giersz & Spurzem 1994

Amaro-Seoane, Freitag & Sp. 2004

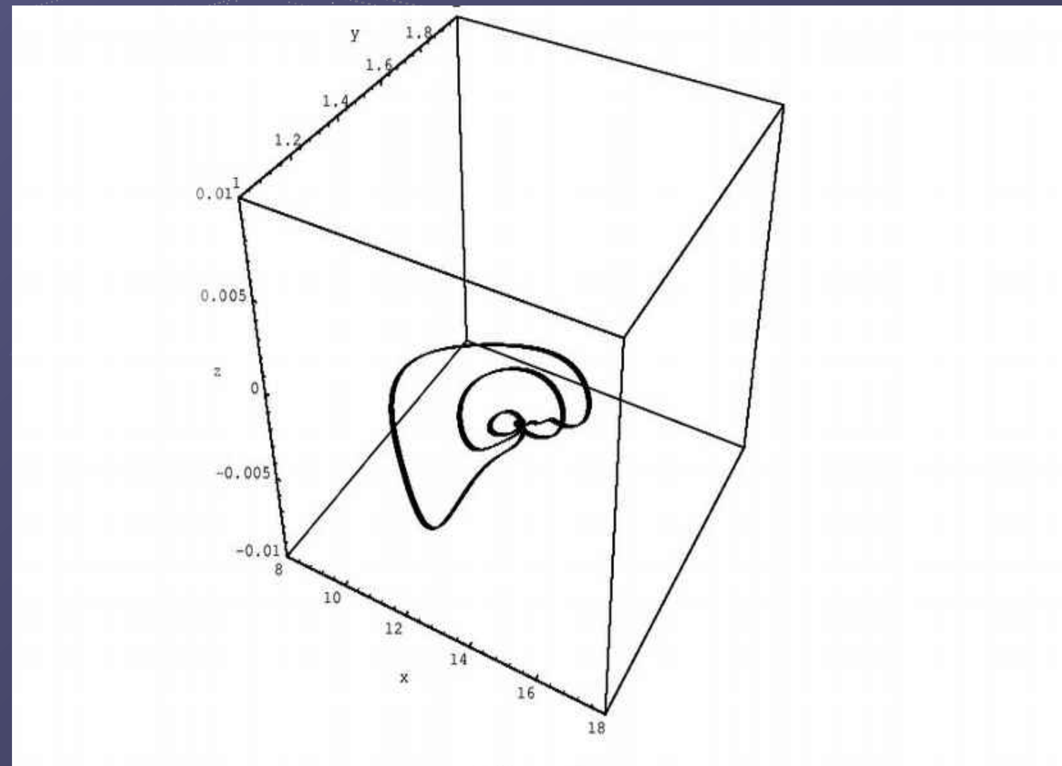

Fig. 3:
Projected three-dimensional attractor for $N = 100.000$ system, $x = \log \rho'_c$, $y = \log \sigma'_c$, $z = \xi$.

Follow-Up of Angeletti & Giannone and Larson

Theoretical Models II: Fokker-Planck

Dissolution of Star Cluster in Tidal Field

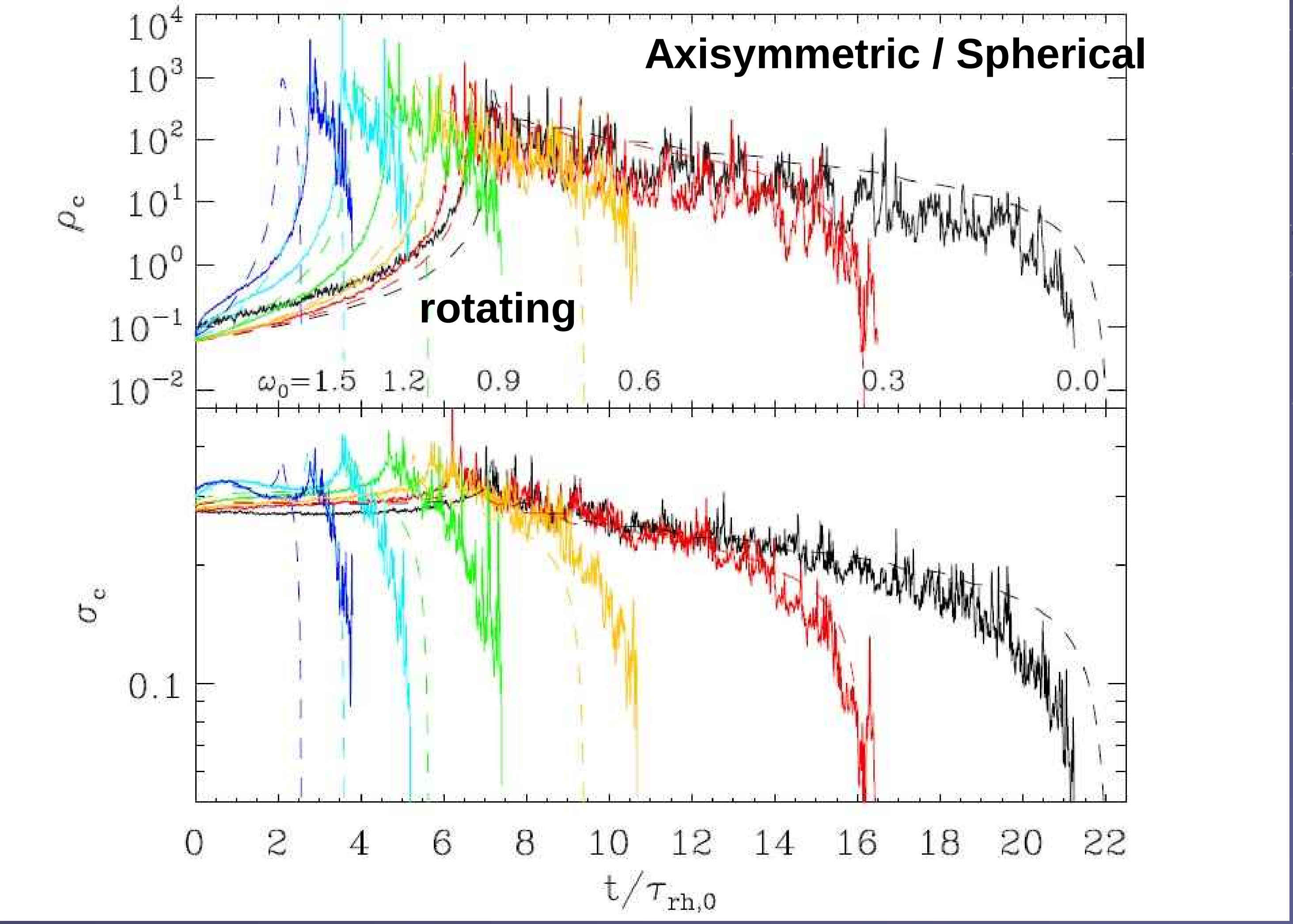

Kim, Yoon, Lee, Spurzem, 2008, MNRAS

Hong, Kim, Lee, Spurzem, 2013, MNRAS

Three Phases in Cluster Dissolution:

1) Core Collapse (Encounters)

2) Post-Collapse Steady Evaporation (Encount)

3) Dynamic final dissolution

Leiden

Key Question 1. When will we see the first star-by-star *N*-body model of a globular cluster?

Douglas Heggie 2010., Leiden
Bottle of Whisky for Million Body Simulation

- Honest N-body simulation
- Reasonable mass at 12 Gyr ($\sim 5 \times 10^4 M_\odot$)
- Reasonable tide (circular galactic orbit will do)
- Reasonable IMF (e.g. Kroupa)
- Reasonable binary fraction (a few percent)
- Any initial model you like (Plummer will do)
- A submitted paper (astro-ph will do)

An inducement: a bottle of single malt Scotch whisky worth €50

Awarded to Long Wang MODEST15s Kobe
See his talk tomorrow

There are low-mass outlying clusters which have lost little mass. They do not count.

Leiden

CPU/GPU N-body6++

Key Question 1. When will we see the first star-by-star *N*-body model of a globular cluster?

- Honest N-body simulation
- Reasonable mass at 12 Gyr ($\sim 5\times10^{4} M_{\odot}$)
- Reasonable tide (circular galactic orbit will do)
- Reasonable IMF (e.g. Kroupa)
- Reasonable binary fraction (a few percent)
- Any initial model you like (Plummer will do)
- A submitted paper (astro-ph will do)

An inducement: a bottle of single malt Scotch whisky worth €50

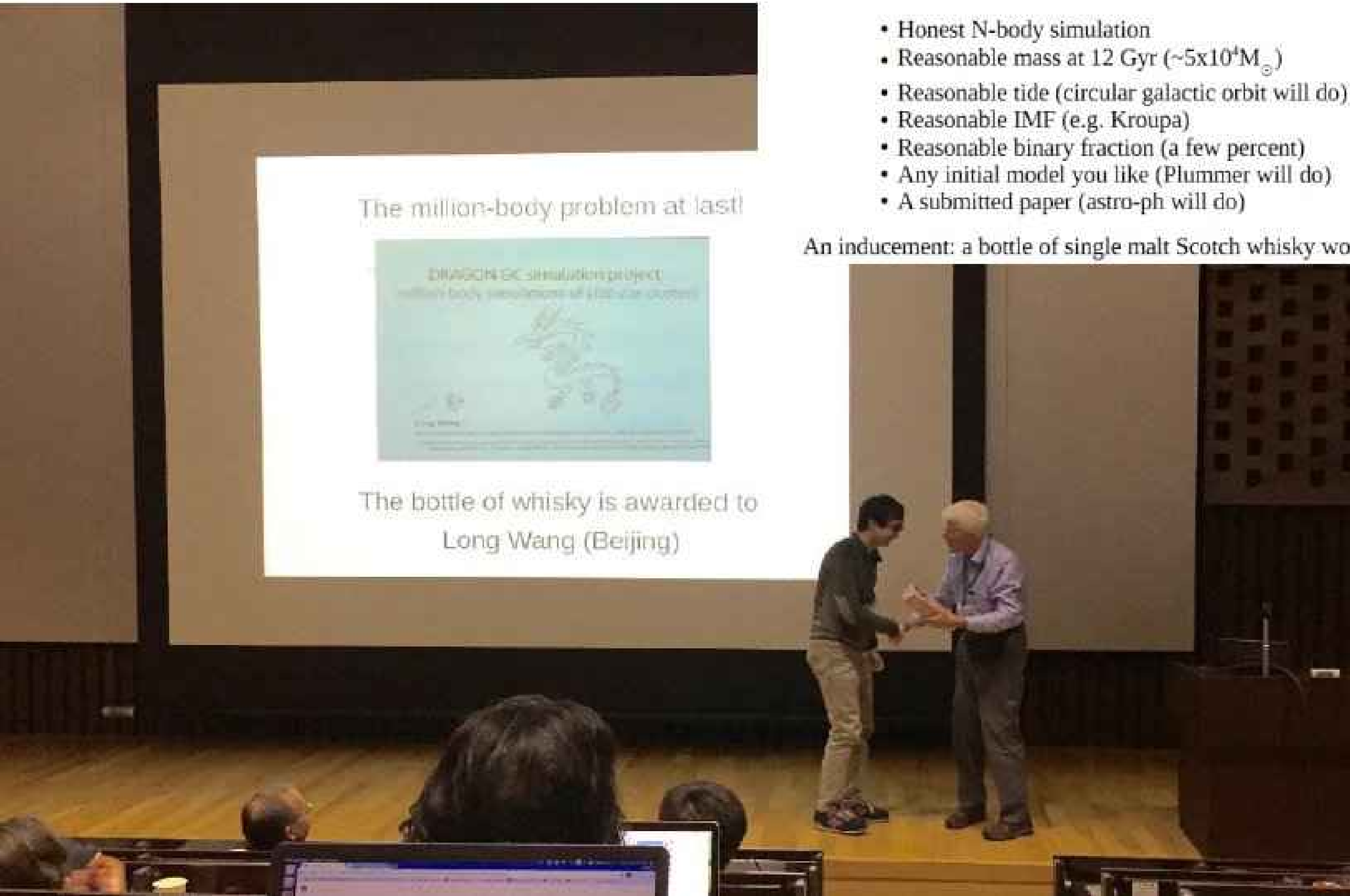

DRAGON Simulation

http://silkroad.bao.ac.cn/dragon/

One million stars direct simulation,

biggest and most realistic direct N-Body simulation of globular star clusters.
With stellar mass function, single and binary stellar evolution, regularization of close encounters, tidal field (NBODY6++GPU).
(NAOC/Silk Road/MPA collaboration).

Wang, Spurzem, Aarseth, Naab et al. MNRAS, 2015

Wang, Spurzem, Aarseth Naab, et al. re-subm. MNRAS 2016

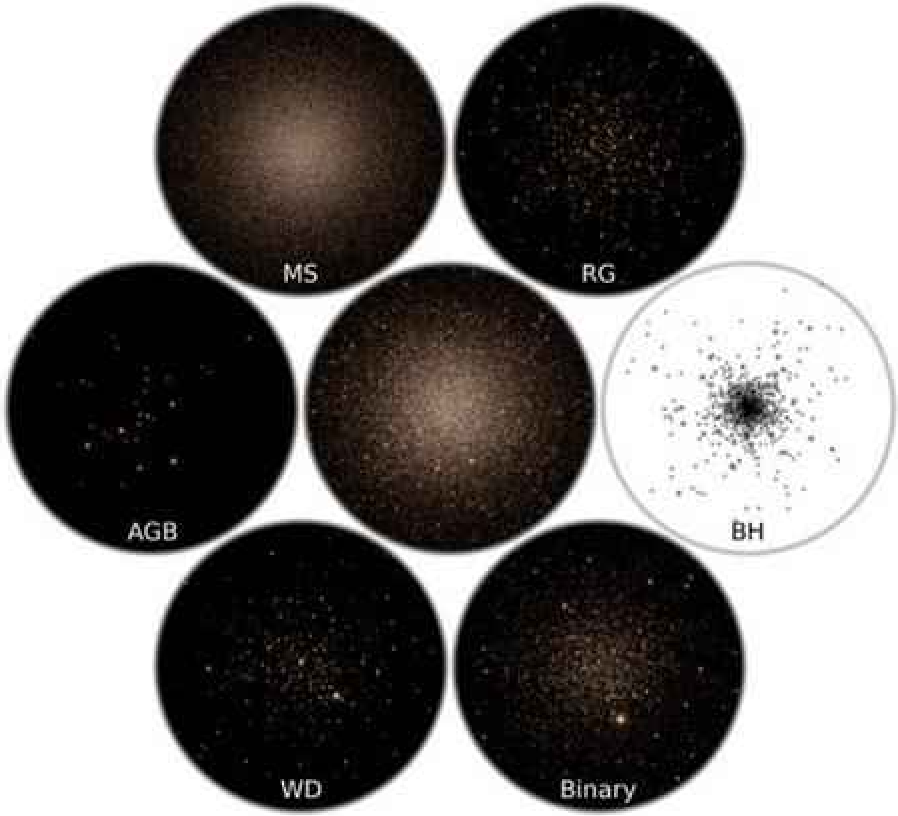

天龙星团模拟：百万数量级恒星、黑洞和引力波

Dragon Star Cluster Simulations: Millions of Stars; black holes and gravitational waves

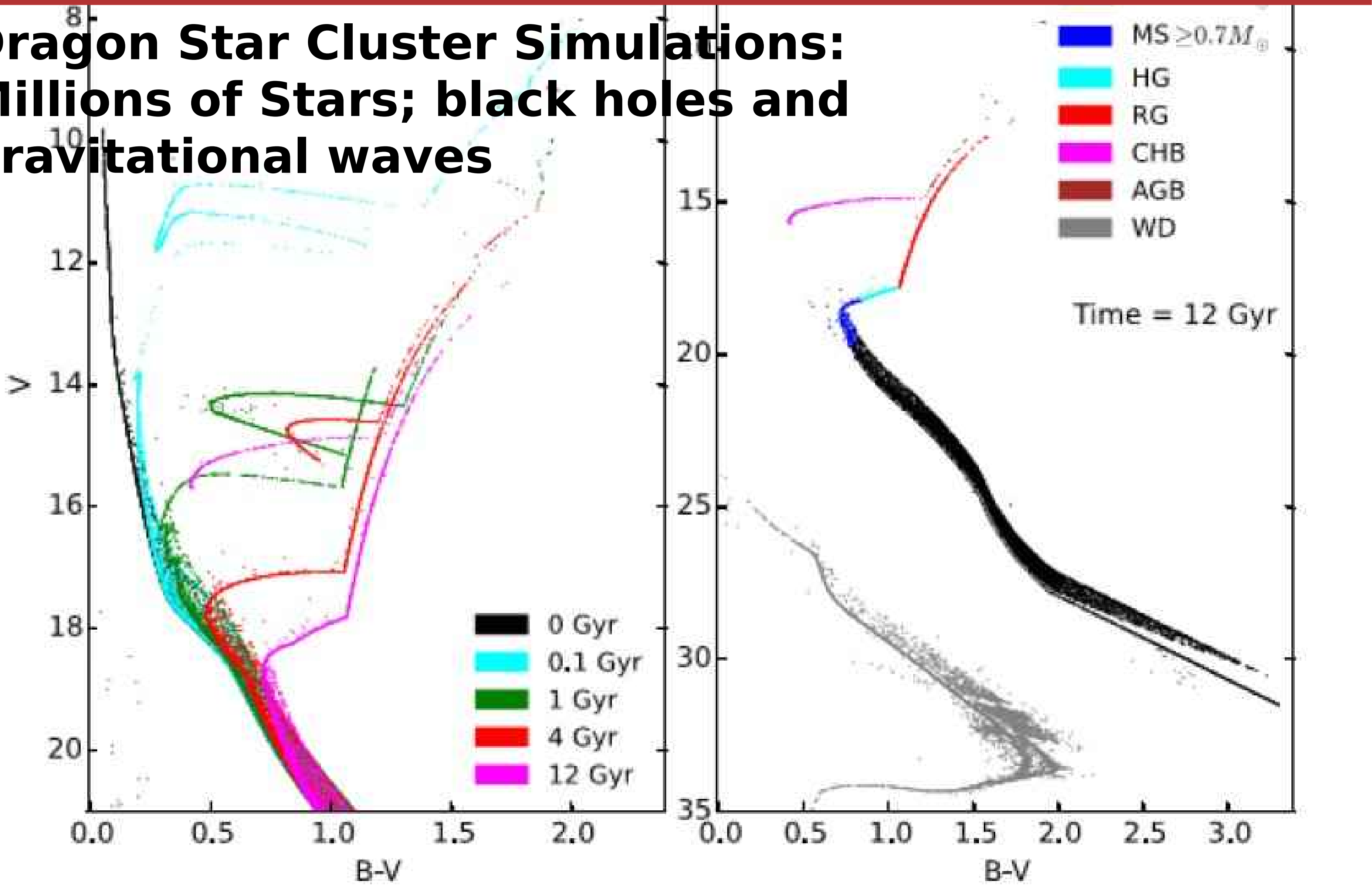

Example: DRAGON vs. Observation of NGC4372...

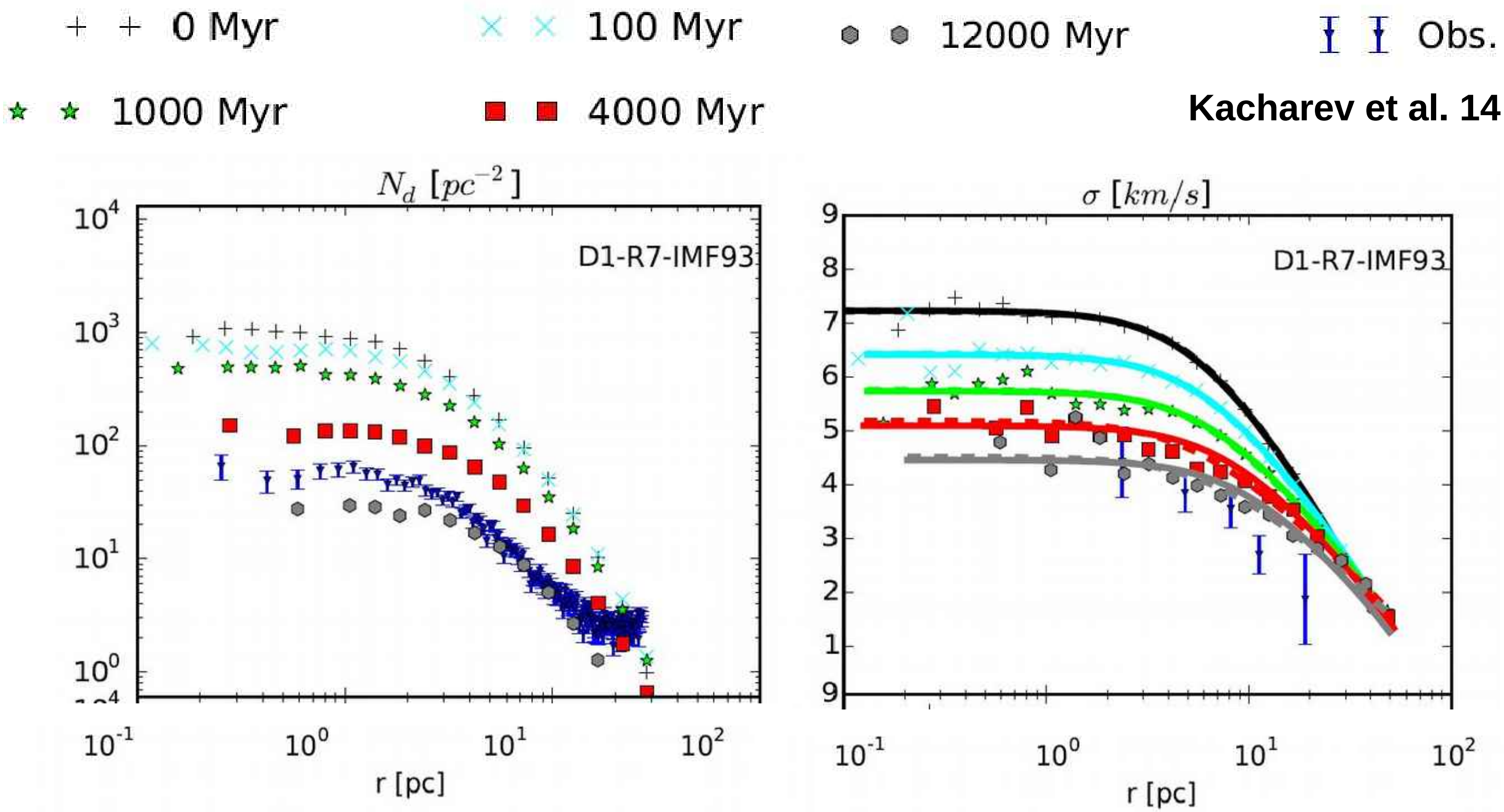

Kacharev et al. 14

GalevNB: a conversion from N-BODY simulations to observations

Xiaoying Pang[1,2,5], Christoph Olczak[1,3], Difeng Guo[1,3], Rainer Spurzem[1,4,3,6] and Ralf Kotulla[7]

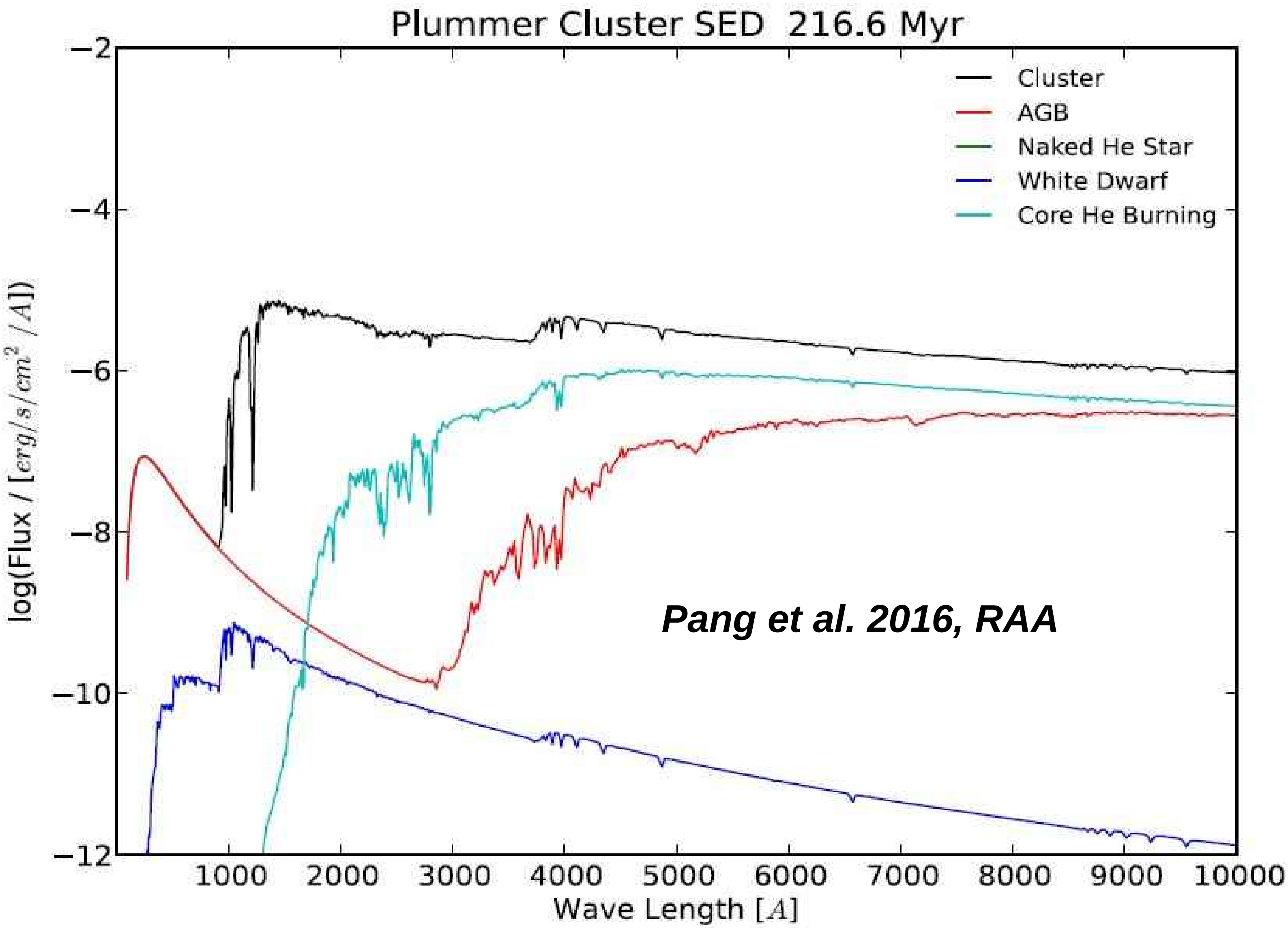

Individual Time Step Storage Scheme for Astrophysical N-body Simulations and its Applications

ApJS 2015

Maxwell Xu Cai (蔡栩)[1,2], Yohai Meiron[2,1], M.B.N. Kouwenhoven[2],

P. Assmann[3,1], Rainer Spurzem[1,2,4]

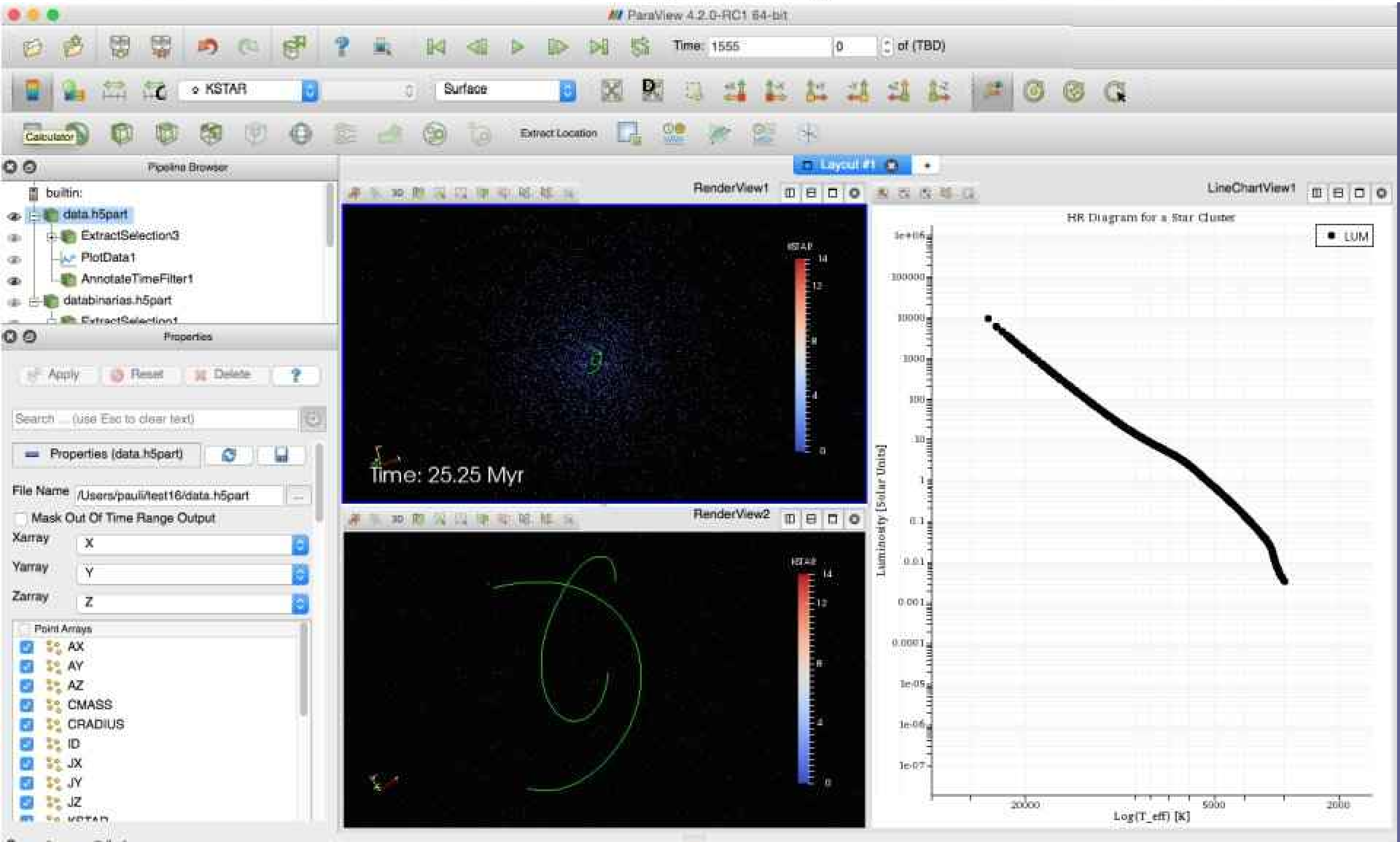

Stardisk Project – Beijing – Almaty – Kiev - Heidelberg

Just, ... Berczik, Spurzem, et a, 2012, ApJ (Paper I)
Kennedy, Meiron et al. 2016 MNRAS (Paper II)
Panamarev, Shukirgaliev et al. 2017 in prep. (Paper III)

The presence of a gaseous accretion disk near an SMBH enhances the mass growth rate of SMBH and forms a compact stellar disk.

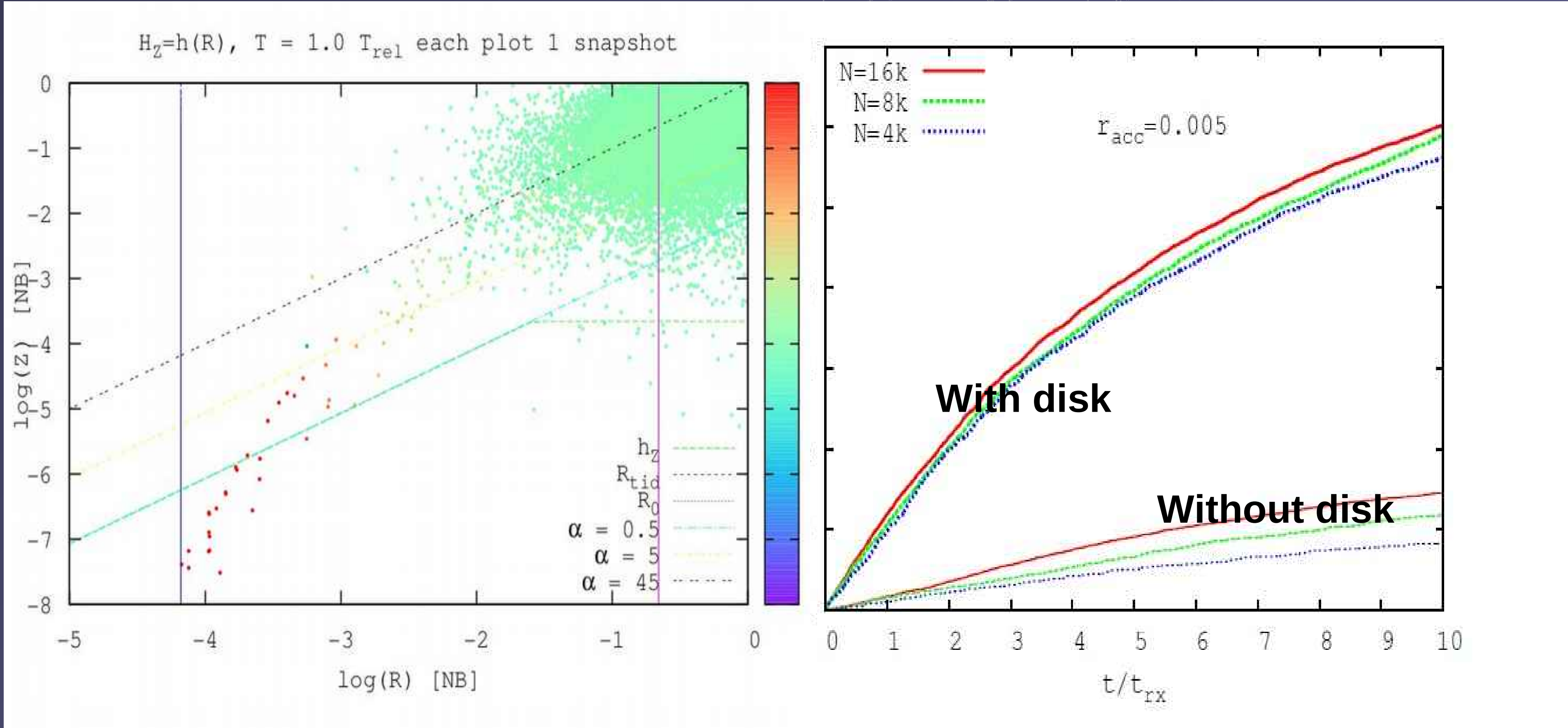

- **Instruments (Hardware/Software)**
- **Dragon Simulations of Star Clusters**
- **Black Holes / Gravitational Waves**

Post-Newtonian Dynamics

Method A: use geodetic equations, harmonic gauge, directly obtain eqs. of motion (Blanchet et al.)
Method B: Hamiltonian approach using ADM gauge (Schaefer et al.)

A and B equivalent till PN2.5 (1/c5), higher order gauge functions appear.**

$$\frac{dv^i}{dt} = -\frac{Gm}{r^2}\left[(1+\mathcal{A})\,n^i + \mathcal{B}\,v^i\right] + \mathcal{O}\left(\frac{1}{c^8}\right), \qquad (181)$$

and find [43] that the coefficients $\mathcal{A}$ and $\mathcal{B}$ are

$$\mathcal{A} = \frac{1}{c^2}\left\{-\frac{3\dot{r}^2\nu}{2} + v^2 + 3\nu v^2 - \frac{Gm}{r}(4+2\nu)\right\}$$

Perihel shift

$$+\frac{1}{c^4}\left\{\frac{15\dot{r}^4\nu}{8} - \frac{45\dot{r}^4\nu^2}{8} - \frac{9\dot{r}^2\nu v^2}{2} + 6\dot{r}^2\nu^2 v^2 + 3\nu v^4 - 4\nu^2 v^4 \right.$$
$$\left. + \frac{Gm}{r}\left(-2\dot{r}^2 - 25\dot{r}^2\nu - 2\dot{r}^2\nu^2 - \frac{13\nu v^2}{2} + 2\nu^2 v^2\right) + \frac{G^2m^2}{r^2}\left(9 + \frac{87\nu}{4}\right)\right\}$$

... higher order...

$$+\frac{1}{c^5}\left\{-\frac{24\dot{r}\nu v^2}{5}\frac{Gm}{r} - \frac{136\dot{r}\nu}{15}\frac{G^2m^2}{r^2}\right\}$$

Grav. Radiation

Post-Newtonian Dynamics

Indirect Proof by Hulse and Taylor, binary pulsar (Nobel prize 1993)

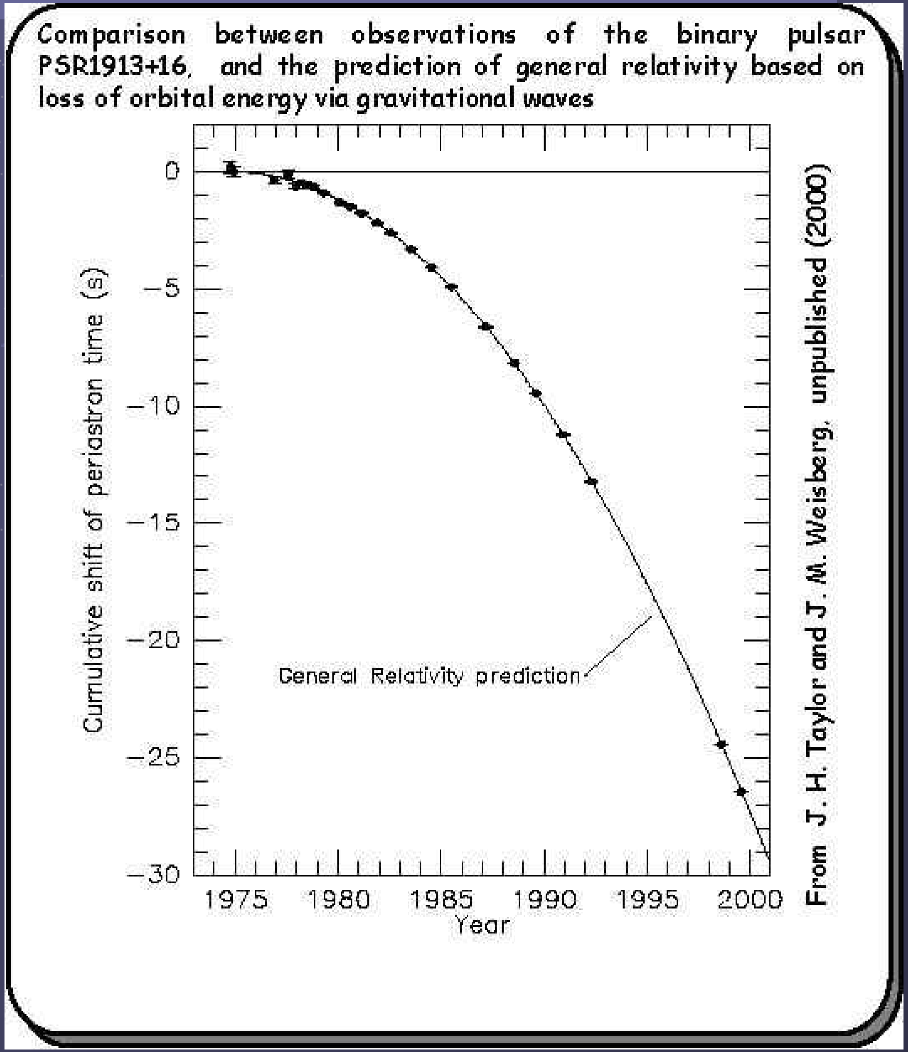

Post-Newtonian Dynamics

Spin-Orbit Interaction S / Spin-Spin SS

$$\frac{d\mathbf{v}_1}{dt} = \mathbf{A}_{\mathrm{N}} + \frac{1}{c^2}\mathbf{A}_{1\mathrm{PN}} + \frac{1}{c^3}\underset{\mathrm{S}}{\mathbf{A}}_{1.5\mathrm{PN}} + \frac{1}{c^4}\left[\mathbf{A}_{2\mathrm{PN}} + \underset{\mathrm{SS}}{\mathbf{A}}_{2\mathrm{PN}}\right] + \frac{1}{c^5}\left[\mathbf{A}_{2.5\mathrm{PN}} + \underset{\mathrm{S}}{\mathbf{A}}_{2.5\mathrm{PN}}\right] + \mathcal{O}\left(\frac{1}{c^6}\right). \qquad (5.1)$$

Faye, Blanchet, Buonanno 2006

$$\underset{\mathrm{S}}{\mathbf{A}}_{1.5\mathrm{PN}} = \frac{Gm_2}{r_{12}^3}\left\{\left[6\frac{(S_1, n_{12}, v_{12})}{m_1} + 6\frac{(S_2, n_{12}, v_{12})}{m_2}\right]\mathbf{n}_{12} + 3(n_{12}v_{12})\frac{\mathbf{n}_{12}\times\mathbf{S}_1}{m_1} + 6(n_{12}v_{12})\frac{\mathbf{n}_{12}\times\mathbf{S}_2}{m_2} - 3\frac{\mathbf{v}_{12}\times\mathbf{S}_1}{m_1} - 4\frac{\mathbf{v}_{12}\times\mathbf{S}_2}{m_2}\right\}. \qquad (5.3a)$$

Post-Newtonian Dynamics

Brem, Amaro-Seoane
Spurzem,
MNRAS 2013

Include
Spin-Orbit
Spin-Spin
PN3, PN3.5
Spin Dynamics

By Patrick Brem
(Diploma Thesis
Univ. Heidelberg)

1PN
2PN + 1.5PN SO
3PN + 2.5PN SO
2.5PN + 2PN SS
3.5PN

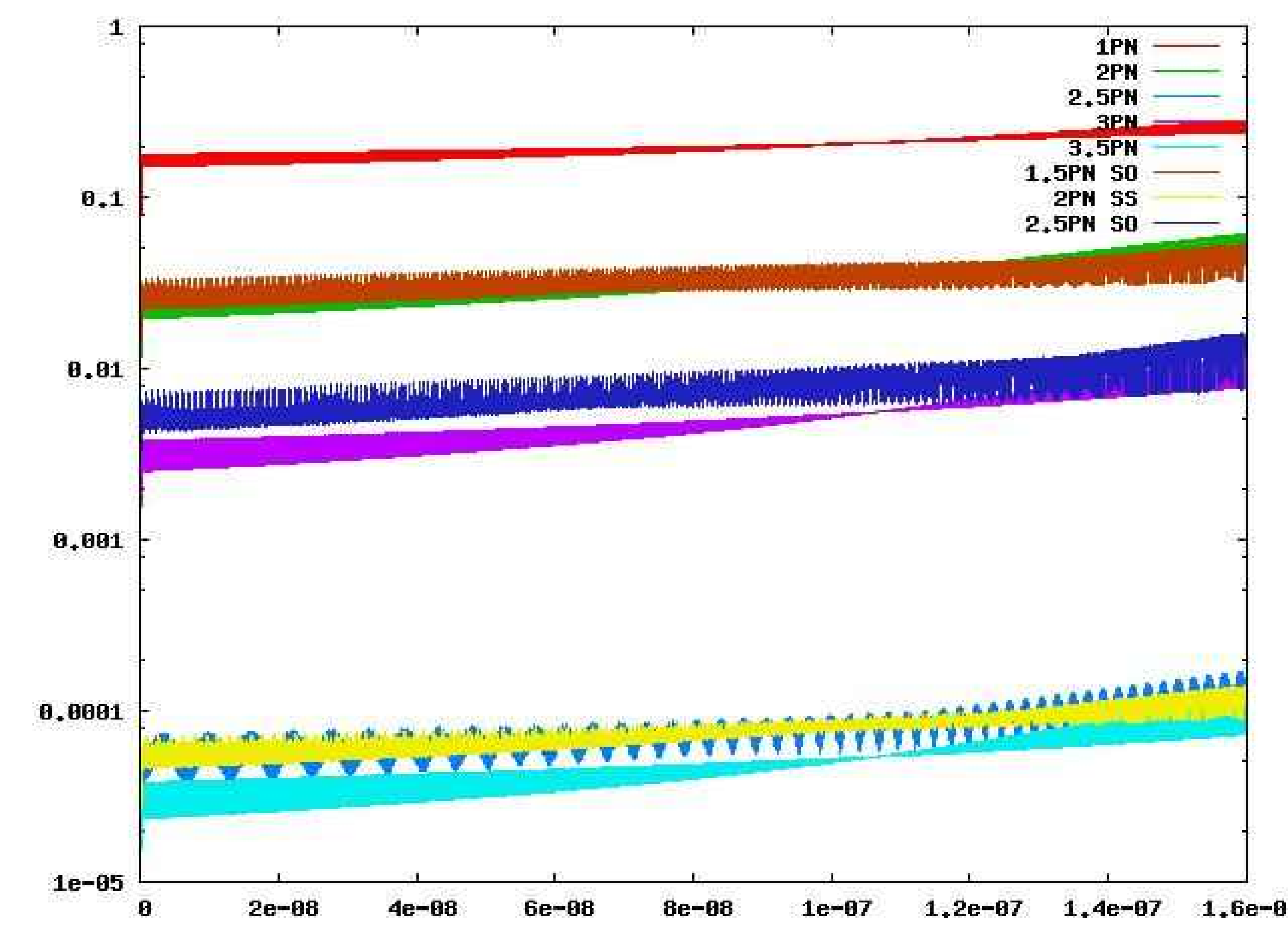

Rezzolla
Final Spin
Formula

Brem,
Amaro-SeoaneS,
Spurzem,
MNRAS 2013

$$|\mathbf{a}_{\rm fin}| = \frac{1}{(1+q)^2}\left[|\mathbf{a}_1|^2 + |\mathbf{a}_2|^2 q^4 + 2|\mathbf{a}_2||\mathbf{a}_1| q^2 \cos\,\alpha + 2(|\mathbf{a}_1|\cos\,\beta + |\mathbf{a}_2| q^2 \cos\,\gamma)|\mathbf{l}|q + |\mathbf{l}|^2 q^2\right]^{1/2},$$

where $q = M_2/M_1$ is the mass ratio and the angles are defined as

$$\cos\,\alpha = \hat{a}_1 \cdot \hat{a}_2, \qquad \cos\,\beta = \hat{a}_1 \cdot \hat{l}, \qquad \cos\,\gamma = \hat{a}_2 \cdot \hat{l}.$$

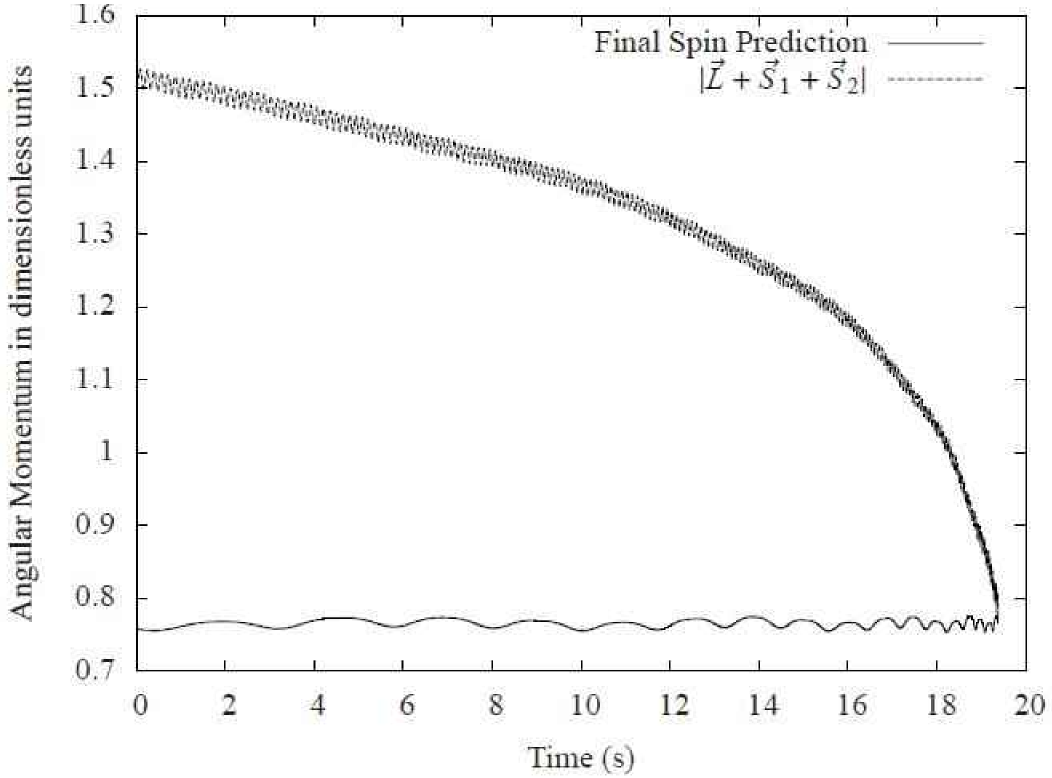

Figure 3.7: Comparison between the current final spin prediction and the actual total angular momentum of the binary system.

Brem, Amaro-Seoane, Spurzem, MNRAS, 2013

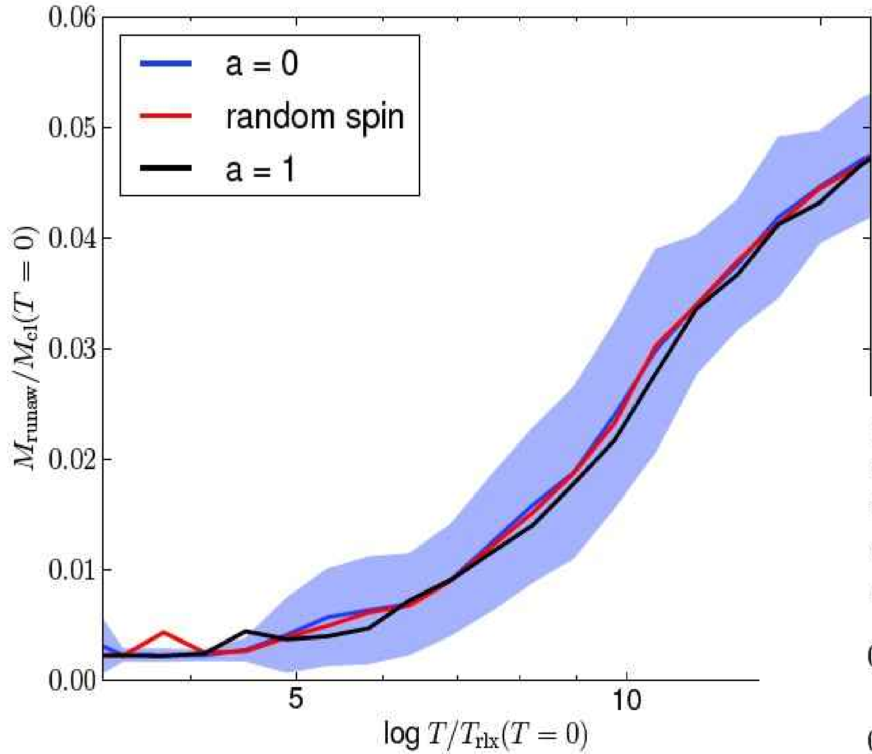

Figure 8. Mass of the runaway body, $M_{\rm runaw}$, for each setup, averaged over 500 runs. $M_{\rm cl}(T = 0)$ is the total mass of the cluster at the time $T = 0$ and $T_{\rm rlx}(T = 0)$ the initial relaxation time of the cluster. The shaded area shows the standard deviation for the $a = 0$ case.

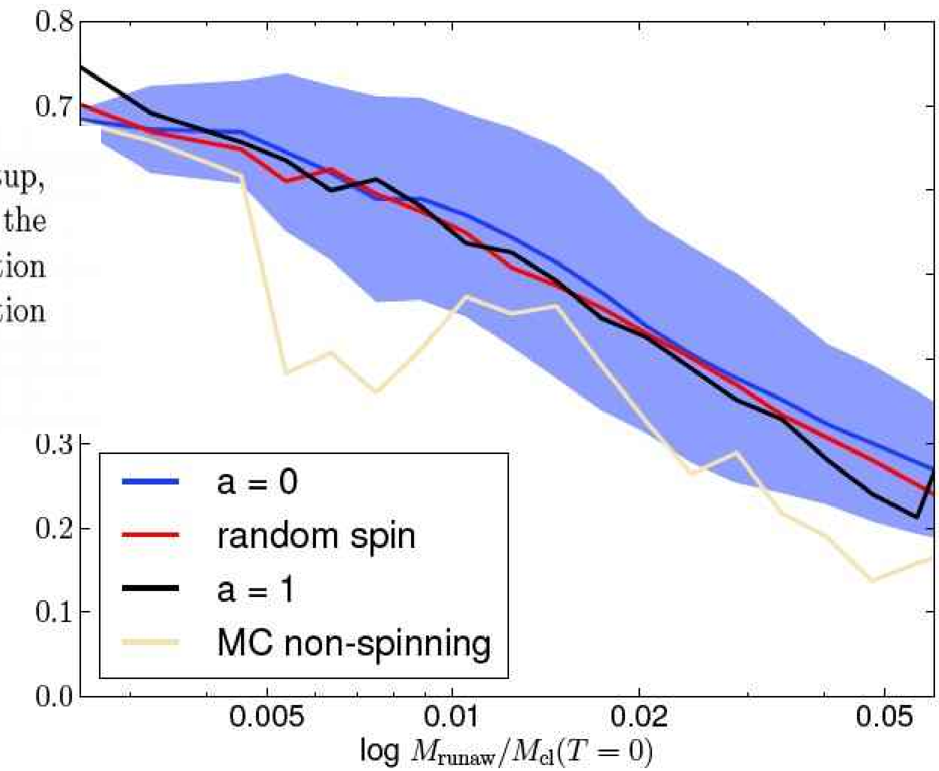

Figure 9. Spin of the runaway body in each simulation, averaged over 500 runs. The shaded area shows the standard deviation for the $a = 0$ case. All initial spin setups lead to a similar evolution, except for the very first data point which is slightly higher for the maximally spinning initial conditions.

MO

Post-Newtonian Dynamics Gravitational Wave Templates

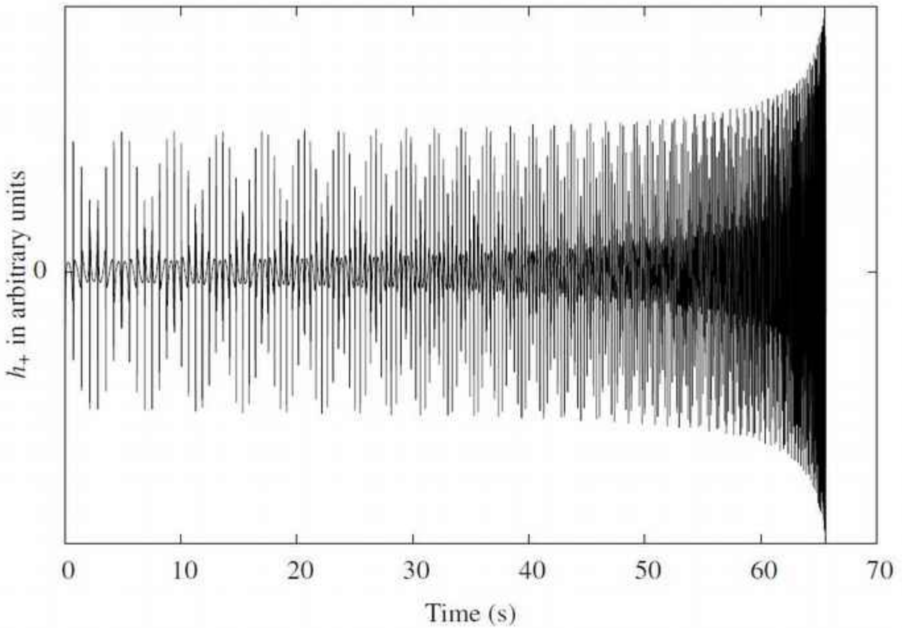

Figure 3.11: Waveform for two equal mass objects on a an orbit with $e = 0.5$.

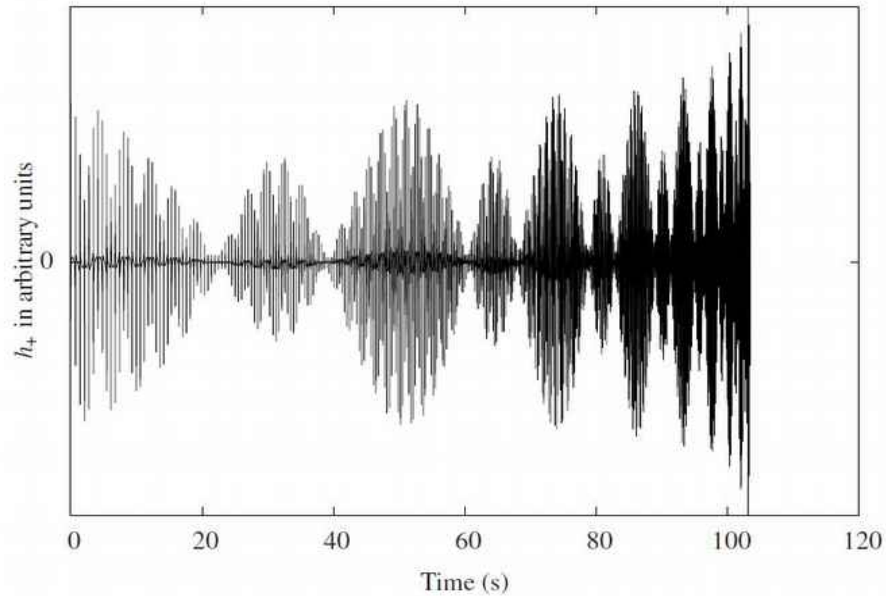

Figure 3.12: Waveform for two objects with a mass ratio of $q = 1/10$ on an orbit with $e = 0.5$ and spins $a_{1,x} = 1.0$, $a_{2,y} = 1.0$.

Handle spin-orbit and spin-spin coupling (P.Brem, R. Spurzem, Univ. Heidelberg)

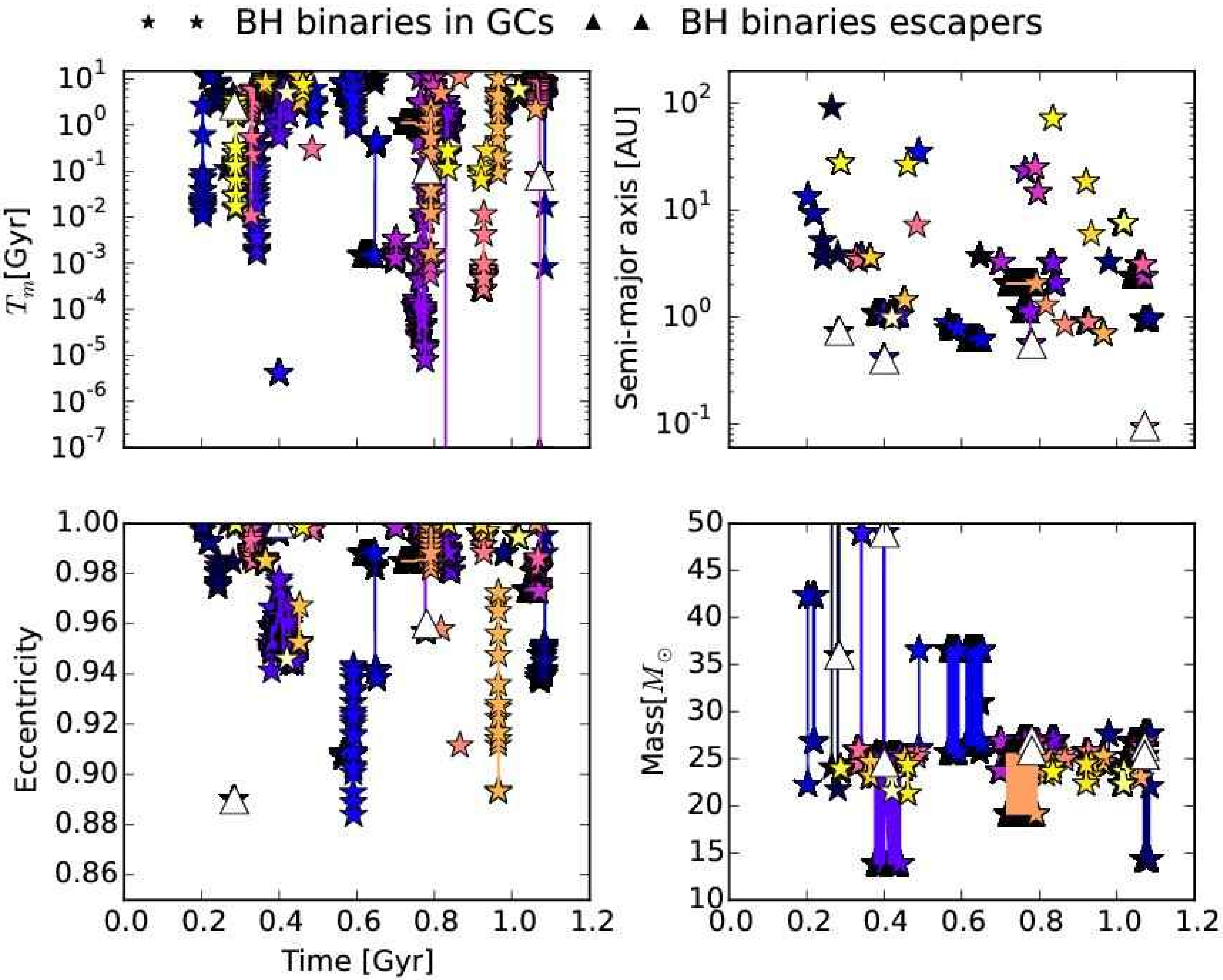

BH binaries in GCs
BH binaries escapers
T_m[Gyr]
Semi-major axis [AU]
Eccentricity
Mass[$M_\odot$]
Time [Gyr]

Example Detections in one of the Dragon models....

Table header:

Status T[Gyr] Name1 Name2 M1[M_sun] M2[M_sun] a[AU] ecc Tm[Gyr] Tme[Gyr]

R7-IMF93 model

2 mergers in GC, 4 escapers:

1. There are two mergers in GCs [P] (merging time scale is very short)

Status	T[Gyr]	Name1	Name2	M1[M_sun]	M2[M_sun]	a[AU]	ecc	Tm[Gyr]	Tme[Gyr]
P	2.32566	49	100229	25.6495	26.3923	12.51693	0.999867	6.18E-05	0.000124
P	1.54318	100237	100373	26.1701	21.932	8.93532	0.99996	3.06E-07	6.13E-07

2. There are two escaped mergers [E]: ('L' means the parameter before ejection)

Status	T[Gyr]	Name1	Name2	M1[M_sun]	M2[M_sun]	a[AU]	ecc	Tm[Gyr]	Tme[Gyr]
L	1.3261	100246	37	25.7717	27.5506	1.088842	0.96292	1.19077	2.239183
E	1.32673	100246	37	25.8	27.6	1.092081	0.96	1.563829	2.925774
L	1.24649	100217	100291	26.9635	24.2528	2.375981	0.987629	0.655226	1.286116
E	1.24711	100217	100291	27	24.3	2.404434	0.99	0.3247471	0.640051

The Observed LIGO Events – Slide from Brown's Talk at KITP (2)

	GW150914	GW151226	LVT151012
Source Mass 1	$36.2^{+5.2}_{-3.8}\ M_\odot$	$14.2^{+8.3}_{-3.7}\ M_\odot$	$23^{+18}_{-6}\ M_\odot$
Source Mass 2	$29.1^{+3.7}_{-4.4}\ M_\odot$	$7.5^{+2.3}_{-2.3}\ M_\odot$	$13^{+4}_{-5}\ M_\odot$
Luminosity Distance	420^{+150}_{-180} Mpc	440^{+180}_{-190} Mpc	1000^{+500}_{-500} Mpc

Abbott, ..., DAB, et al. arXix:1606.04856

GW Detection Frequency Time Diagram

Top: Our simulation (Sobolenko , Veles, Wang, Berczik, Spurzem, et al. In prep

Down: Abott et al. 2016 LIGO measurement

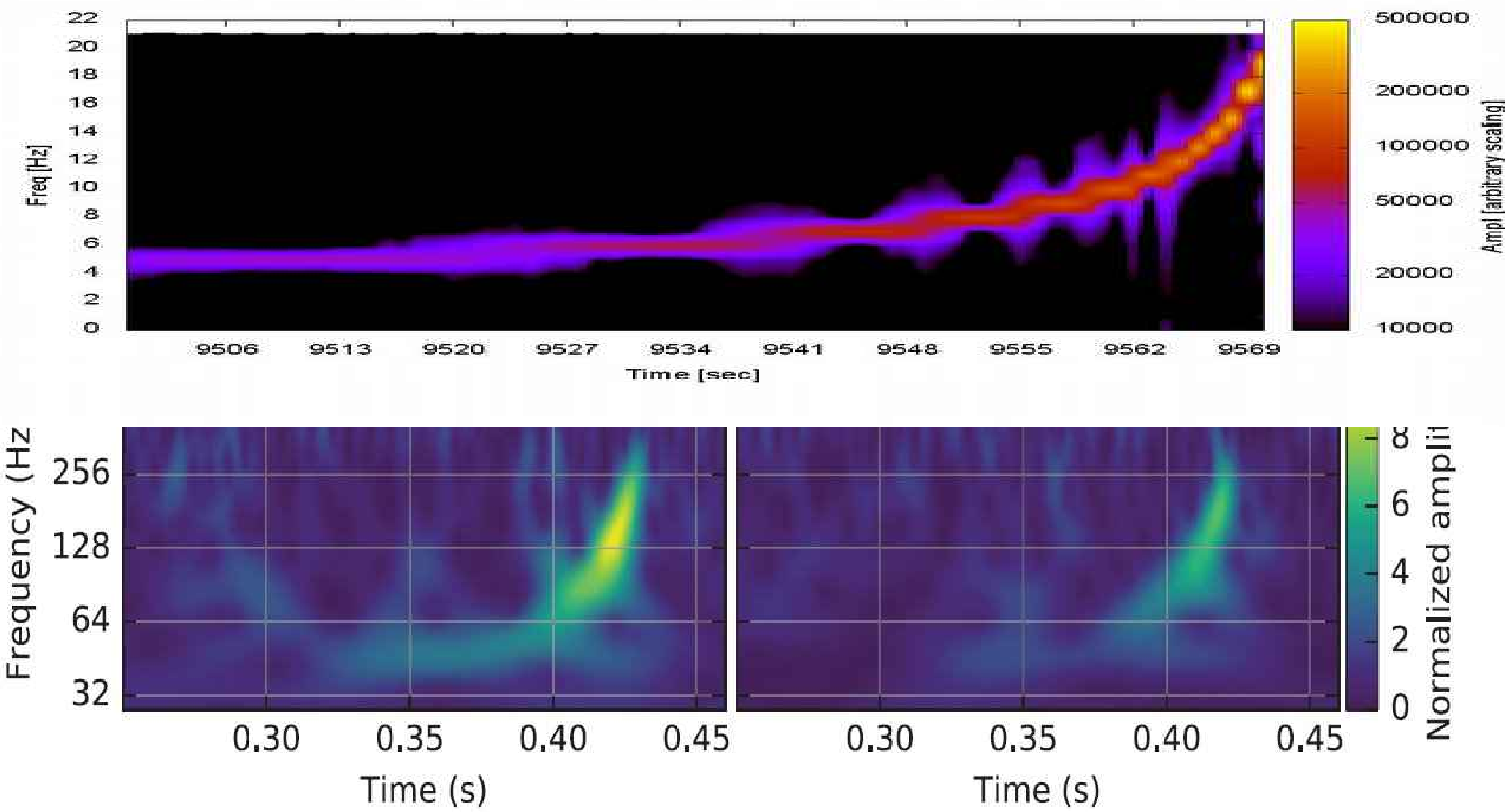

FIG. 1. The gravitational-wave event GW150914 observed by the LIGO Hanford (H1, left column panels) and Livingston (L1, right

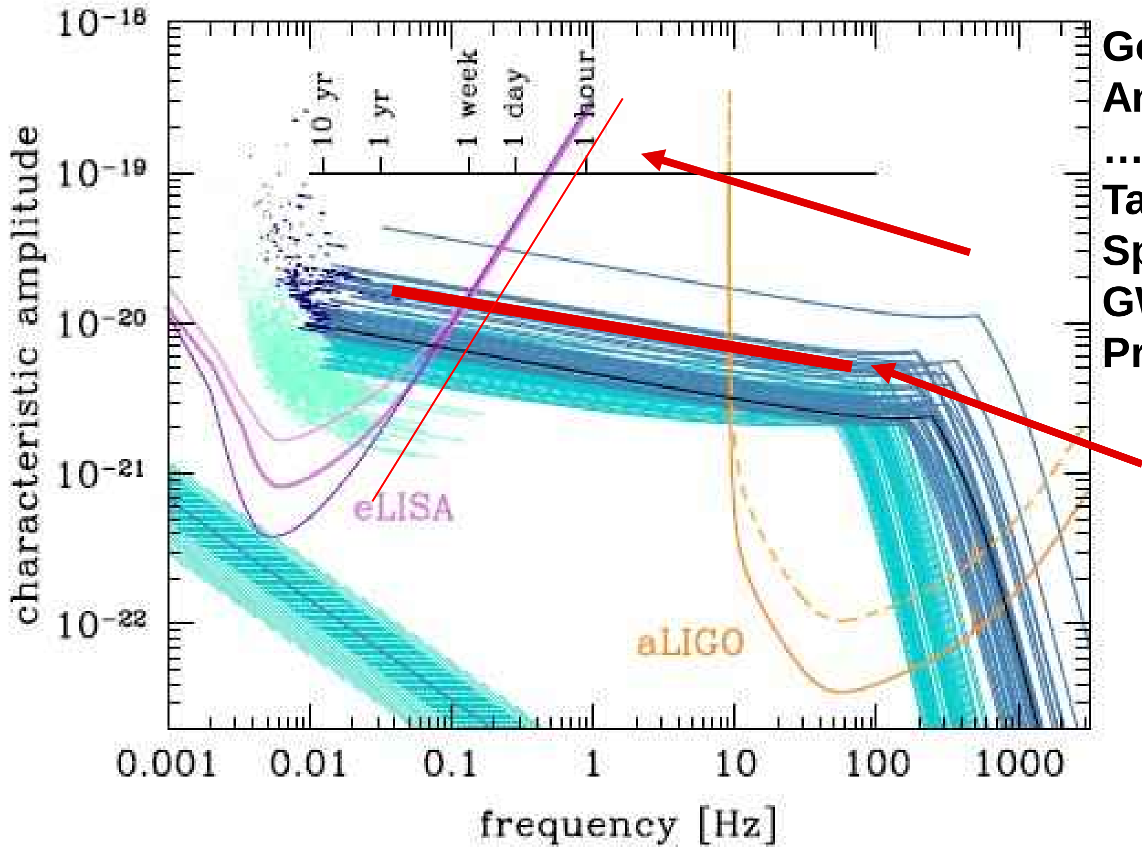

Gong, Lau, …
Amaro-Seoane,
…Spurzem + 2015
Taiji Chinese
Space Based
GW Detector
Proposal

“Our”
DRAGON
Black Hole
Binary

Sesana 2016

FIG. 1: The multi-band GW astronomy concept. The violet lines are the total sensitivity curves (assuming two Michelson) of three eLISA configurations; from top to bottom N2A1, N2A2, N2A5 (from [11]). The orange lines are the current (dashed) and design (solid) aLIGO sensitivity curves. The lines in different blue flavours represent characteristic amplitude tracks of BHB sources for a realization of the *flat* population model (see main text) seen with S/N> 1 in the N2A2 configuration (highlighted as the thick eLISA middle curve), integrated assuming a five year mission lifetime. The light turquoise lines clustering around 0.01Hz are sources seen in eLISA with S/N< 5 (for clarity, we down-sampled them by a factor of 20 and we removed sources extending to the aLIGO band); the light and dark blue curves crossing to the aLIGO band are sources with S/N> 5 and S/N> 8 respectively in eLISA; the dark blue marks in the upper left corner are other sources with S/N> 8 in eLISA but not crossing to the aLIGO band within the mission lifetime. For comparison, the characteristic amplitude track completed by GW150914 is shown as a black solid line, and the chart at the top of the figure indicates the frequency progression of this particular source in the last 10 years before coalescence. The shaded area at the bottom left marks the expected confusion noise level produced by the same population model (median, 68% and 95% intervals are shown). The waveforms shown are second order post-Newtonian inspirals phenomenologically adjusted with a Lorentzian function to describe the ringdown.

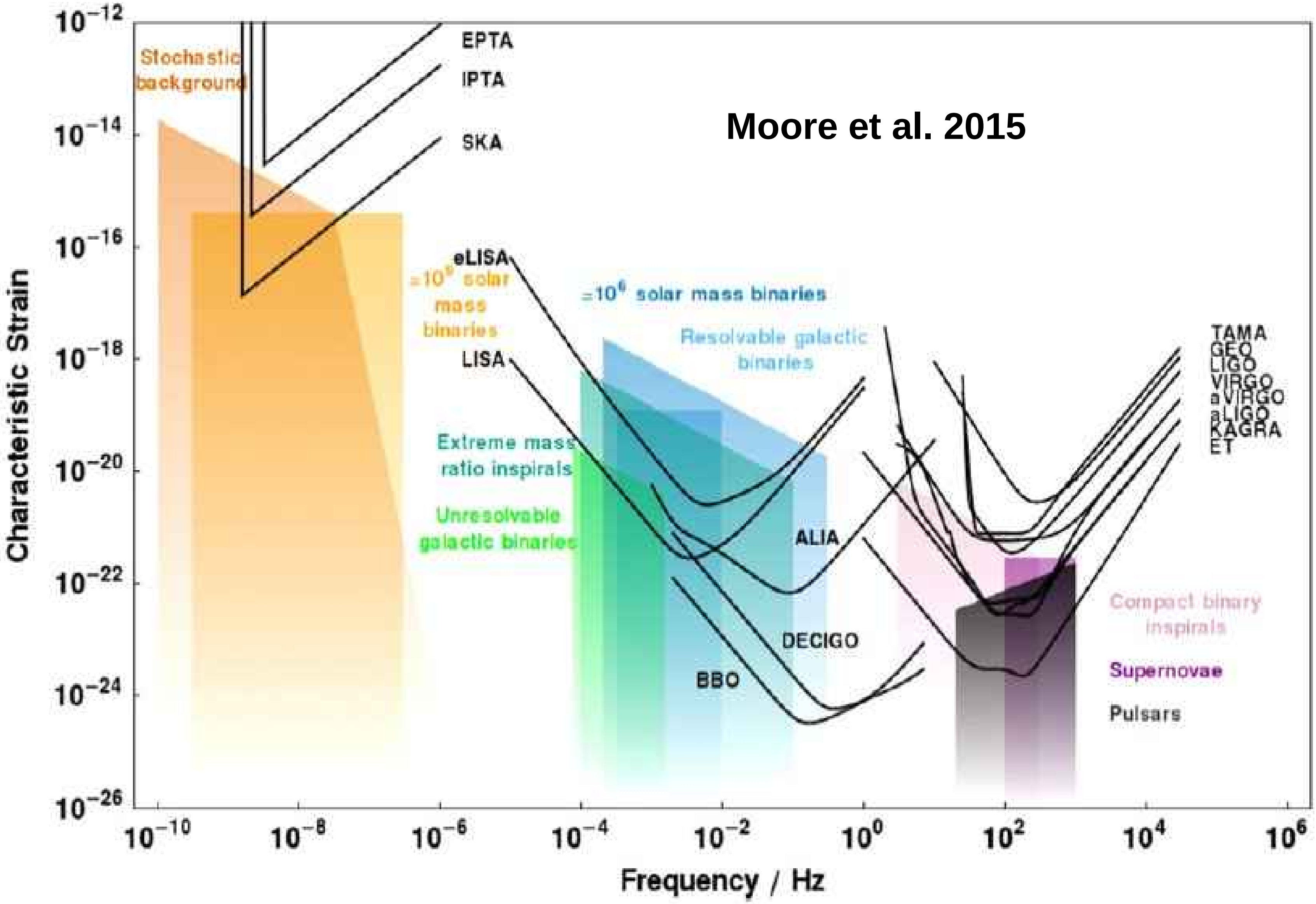

Figure A1. A plot of characteristic strain against frequency for a variety of detectors and sources.

Summary

- **Astrophysical High Precision N-Body – Star Clusters**

  DRAGON simulations of low-density star cluster

  Need more Dragon simulations to study physics of rotation, binaries, high density, nuclear star clusters

(Wang et al. 2015a, ApJ, 2015b, Cai et al. 2015, ApJS, Pang et al. 2015 RAA, Huang et al. 2015, RAA)

Black Holes in Galactic Nuclei → see

(Zhong et al. 2014, 2015, ApJ. Li et al. 2012 ApJ, 2015 subm. ApJ Khan et al. 2012, 2014 ApJ, Sobolenko et al. 2015, Berczik et al. 2016)

- **Further Astrophysical Science Drivers:**

  Extragalactic and Massive Star Clusters

  IMBH Formation? Multiple Generations?

  Gravitational Waves in Pulsar Timing/eLISA/LIGO

  Radio Pulsars

  Accretion to central black holes

NAOC 中国科学院国家天文台 NATIONAL ASTRONOMICAL OBSERVATORIES ,CHINESE ACADEMY OF SCIENCES

北京大学 PEKING UNIVERSITY

INVITATION/DISCUSSION

- Building National and International Community on on Astrophysical GPU Supercomputing in China and Partner countries (e.g. South Africa, Pakistan, Chile...)

- Training and Teaching – come to Beijing (NAOC) for testing and developing, or remote testing/running, or invite our experts for talks and hardware/software cooperation (regular schools and training workshops
  http://kiaa.pku.edu.cn/~kouwenhoven/nbody.html
  And GPU lectures.

- Relation to 'big data' – common platforms for pathfinding/testing with simulations?

N-Body – Monte Carlo Comparison II
Wang, Askar, Giersz, Spurzem, 2016, in prep.

Binary Black Holes versus
Time (left)
Radius (right)
In DRAGON clusters

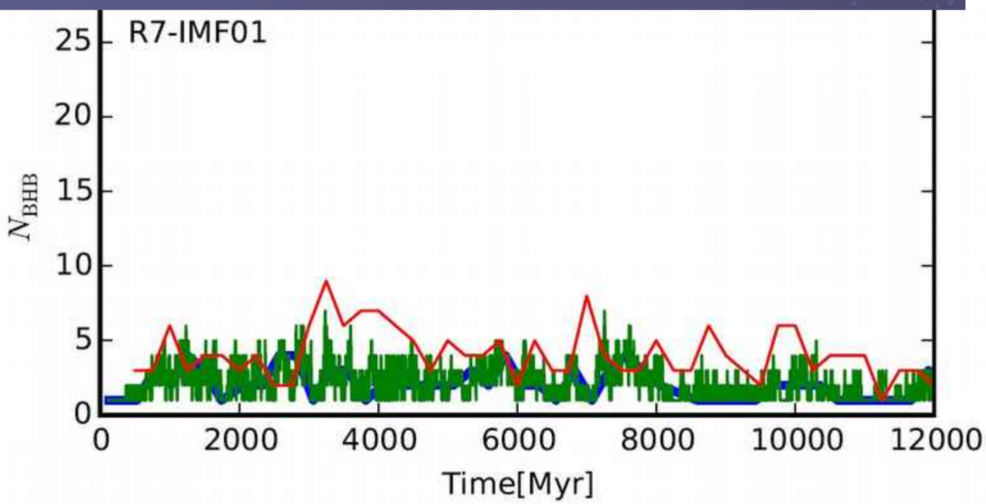

Figure 2. The evolution of hard BHB ($\tilde{a}$ < 100 AU) numbers within core radii in R7-IMF93 ($R_c = 2pc$) and R7-IMF01 ($R_c = 3pc$). The blue curves show direct N-body (NBODY6++GPU) results and red curves show Monte-Carlo (MOCCA) results. These two curves have a same time resolution. The green curves show the same direct N-body result but higher time resolution.

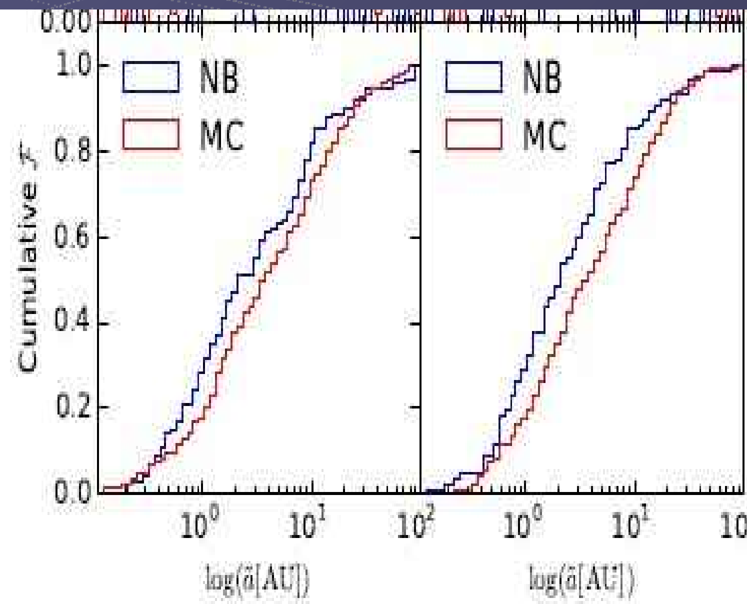

Figure 3. The normalized distribution of hard BHB scaled-semi-major axises $\tilde{a}$ ($\tilde{a}$ < 100 AU) within core radii in R7-IMF93 and R7-IMF01 models. The upper panels show the histograms and the lower panels show the cumulative distributions. To obtain better statistics, BHB data from snapshots of every 250 Myr between the ages of 1 Gyr and 12 Gyr are collected (totally 45 snapshots). The blue color indicates the direct N-body results and the red color indicates the Monte-Carlo results.